International Journal of Pharmaceutics 658 (2024) 124222

Contents lists available at ScienceDirect

International Journal of Pharmaceutics

journal homepage: www.elsevier.com/locate/ijpharm

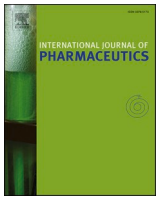

Novel nanostructured lipid carriers loading Apigenin for anterior segment ocular pathologies

L. Bonilla-Vidal [a,b], M. Espina [a,b], M.L. García [a,b], L. Baldomà [c,d], J. Badia [c,d], J.A. González [e], L.M. Delgado [f], A. Gliszczyńska [g], E.B. Souto [h,i], E. Sánchez-López [a,b,j,*]

[a] Department of Pharmacy, Pharmaceutical Technology and Physical Chemistry, University of Barcelona, 08028 Barcelona, Spain
[b] Institute of Nanoscience and Nanotechnology (IN^{2}UB), University of Barcelona, 08028 Barcelona, Spain
[c] Department of Biochemistry and Physiology, University of Barcelona, 08028 Barcelona, Spain
[d] Institute of Biomedicine of the University of Barcelona (IBUB), Institute of Research of Sant Joan de Déu (IRSJD), 08950 Barcelona, Spain
[e] Department of Endodontics, Faculty of Dentistry, International University of Catalonia (UIC), 08195 Barcelona, Spain
[f] Bioengineering Institute of Technology, International University of Catalonia (UIC), 08028 Barcelona, Spain
[g] Department of Food Chemistry and Biocatalysis, Wrocław University of Environmental and Life Sciences, Wrocław, Poland
[h] REQUIMTE/UCIBIO, Laboratory of Pharmaceutical Technology, Department of Drug Sciences, Faculty of Pharmacy, University of Porto, Rua de Jorge Viterbo Ferreira, 228, 4050-313 Porto, Portugal
[i] Associate Laboratory i4HB—Institute for Health and Bioeconomy, Faculty of Pharmacy, University of Porto, 4050-313 Porto, Portugal
[j] Unit of Synthesis and Biomedical Applications of Peptides, IQAC-CSIC, 08034 Barcelona, Spain

ARTICLE INFO

Keywords:
Apigenin
Nanostructured lipid carriers
Rosehip oil
Lipid nanoparticles

ABSTRACT

Dry eye disease (DED) is a chronic multifactorial disorder of the ocular surface caused by tear film dysfunction and constitutes one of the most common ocular conditions worldwide. However, its treatment remains unsatisfactory. While artificial tears are commonly used to moisturize the ocular surface, they do not address the underlying causes of DED. Apigenin (APG) is a natural product with anti-inflammatory properties, but its low solubility and bioavailability limit its efficacy. Therefore, a novel formulation of APG loaded into biodegradable and biocompatible nanoparticles (APG-NLC) was developed to overcome the restricted APG stability, improve its therapeutic efficacy, and prolong its retention time on the ocular surface by extending its release. APG-NLC optimization, characterization, biopharmaceutical properties and therapeutic efficacy were evaluated. The optimized APG-NLC exhibited an average particle size below 200 nm, a positive surface charge, and an encapsulation efficiency over 99 %. APG-NLC exhibited sustained release of APG, and stability studies demonstrated that the formulation retained its integrity for over 25 months. *In vitro* and *in vivo* ocular tolerance studies indicated that APG-NLC did not cause any irritation, rendering them suitable for ocular topical administration. Furthermore, APG-NLC showed non-toxicity in an epithelial corneal cell line and exhibited fast cell internalization. Therapeutic benefits were demonstrated using an *in vivo* model of DED, where APG-NLC effectively reversed DED by reducing ocular surface cellular damage and increasing tear volume. Anti-inflammatory assays *in vivo* also showcased its potential to treat and prevent ocular inflammation, particularly relevant in DED patients. Hence, APG-NLC represent a promising system for the treatment and prevention of DED and its associated inflammation.

1. Introduction

Dry eye disease (DED) or keratoconjunctivitis sicca is one of the most prevalent ocular conditions worldwide and a leading cause of doctor appointments, imposing a significant societal and economic burden (Kumari et al., 2021). Despite its high incidence, its treatment remains unsatisfactory, leading to a diminished quality of life for affected patients. DED is a multifactorial pathology of the ocular surface characterized by the disruption of tear film homeostasis. This disruption is accompanied by ocular symptoms, including tear film instability, hyperosmolarity, ocular surface inflammation and damage, and neurosensory abnormalities, all of which contribute to its etiology (López-

* Corresponding author at: Department of Pharmacy, Pharmaceutical Technology and Physical Chemistry, University of Barcelona, 08028 Barcelona, Spain.
E-mail address: esanchezlopez@ub.edu (E. Sánchez-López).

https://doi.org/10.1016/j.ijpharm.2024.124222
Received 7 March 2024; Received in revised form 23 April 2024; Accepted 9 May 2024
Available online 11 May 2024

Machado et al., 2021; Huang et al., 2021; Craig et al., 2017). Moreover, DED may also be associated with other conditions or medication side effects, and its incidence increases with age (De Paiva, 2017). Topical treatment is the preferred approach for managing DED due to its ease and painlessness of application. Artificial tears, typically administered as eye drops, gels, or ointments, are commonly used to moisturize and lubricate the ocular surface, serving as the first line of treatment. These agents temporarily alleviate symptoms by reducing tear film osmolarity and diluting inflammatory markers. However, they provide only short-term relief, lack anti-inflammatory properties, and do not address the underlying causes of DED (Kelly et al., 2023; Baiula and Spampinato, 2021). For inflammation, conventional marketed drugs, such as corticosteroids and NSAIDs possess anti-inflammatory effects but are associated with serious long-term side effects, such as an increased intraocular pressure and cataract formation (Wei et al., 2023). Cyclosporine, another conventional DED treatment, exhibits immunomodulatory activity, but it can lead to side effects such as ocular burning sensation and itching, among others (Periman et al., 2020; Peng et al., 2022).

In recent years, Apigenin (APG) has emerged as a potential treatment option due to its excellent therapeutic properties. APG has been shown to ameliorate ocular surface lesions and protect the retina from oxidative damage in *in vivo* models (Zhang et al., 2020; Liu et al., 2019). Given the therapeutic potential and safety profile of APG, it represents a promising novel treatment for DED (Liu et al., 2019). However, despite the interest in APG as an ocular treatment, it is hindered by its low solubility and bioavailability (Wang et al., 2019). Due to this fact, novel ocular delivery systems have been developed. One of the most interesting delivery systems are lipid nanoparticles, which offer multiple advantages including decreased toxicity, suitable stability over time, eco-friendly and economical production, easy industrial scale-up, the ability to be autoclaved or sterilized, and increased kinetic stability compared to other drug delivery systems such as liposomes or niosomes (Battaglia et al., 2016). Moreover, the latest generation of lipid nanoparticles, known as nanostructured lipid carriers (NLC), hold promise as an ocular delivery system due to their enhanced stability compared to previous nanoparticles like solid lipid nanoparticles (SLN). This improvement is achieved through the addition of a liquid lipid component. Additionally, the lipids used in NLC formulations can be tailored to provide specific benefits such as hydrating the ocular surface or imparting anti-inflammatory or antioxidant properties (Bonilla et al., 2022).

To increase the stability of APG and enhance its therapeutic efficacy and retention time on the ocular surface, a novel strategy was developed involving encapsulation into biocompatible and biodegradable NLC. This approach aims to achieve prolonged release of APG, thereby minimizing its degradation and maximizing its therapeutic impact on the ocular surface. Furthermore, a liquid lipid with antioxidant, anti-inflammatory, and regenerative properties was chosen: rosehip oil. Extracted from *Rosa canina* seeds, rosehip oil possesses exceptional value due to its rich composition of essential fatty acids, tocopherols, sterols, and phenolic compounds, all of which offer diverse and beneficial functional properties (Kiralan and Yildirim, 2019). Moreover, hyaluronic acid (HA), a naturally occurring anionic polysaccharide with mucomimetic properties, has been incorporated into the formulation. HA ability to prolong precorneal residence time and reduce surface desiccation makes it a valuable viscosity-building agent in ocular delivery devices. It enhances drug retention and alleviates ocular surface dryness (Agarwal et al., 2021). Moreover, to enhance the bioavailability of the formulation upon administration to the ocular mucosa, a cationic lipid has been selected. Cationic lipids promote electrostatic interactions between the positively charged surface of the particles and the negatively charged ocular mucosa, significantly extending drug residence time (Fangueiro et al., 2016). Furthermore, in previous ocular delivery studies, the chosen cationic lipid, dimethyldioctadecylammonium bromide (DDAB), demonstrated no toxicity up to a concentration of 0.5 % (Silva et al., 2019).

As a result, the objective of this research was to develop a novel nanostructured drug delivery system comprising a surface-functionalized cationic HA-coated APG-loaded NLC for the effective treatment of DED. Currently, there is no formulation designed for topical administration containing this composition capable of increase ocular tear volume, reduce inflammation, and improve corneal erosions. Therefore, this work is focused on comprehensive *in vitro* and *in vivo* investigations to evaluate the biocompatibility, therapeutic potential, and anti-inflammatory efficacy of the APG-NLC.

2. Materials and methods

2.1. Materials

APG was acquired from Apollo Scientific (Cheshire, UK). Compritol 888 ATO® (Glyceryl distearate) was gifted by Gattefossé (Madrid, Spain). Tween® 80 (Polysorbate 80), rose Bengal, fluorescein and Nile red (NR) were obtained from Sigma Aldrich (Madrid, Spain). Rosehip oil was acquired from Acofarma Formulas Magistrales (Barcelona, Spain). DDAB was purchased to TCI Europe (Zwijndrecht, Belgium). HA was gifted by Bloomage Freda Biopharm (Jinan, China). All the others reagents used in this research were of analytical grade. Purified water was obtained by a Millipore Milli-Q Plus system.

2.2. APG-NLC preparation and optimization

APG-NLC production was performed using the hot high-pressure homogenization method (Homogenizer FPG 12800, Stansted, United Kingdom). Briefly, an initial emulsion was prepared by mixing the compounds using an Ultraturrax T25 (IKA, Germany) at 8000 rpm for 30 s. The fabrication conditions included a temperature of 85 °C, three homogenization cycles and 900 bars of pressure (Carvajal-Vidal et al., 2019). The formulation was previously optimized (Bonilla-Vidal et al., 2023), and increasing amounts of a cationic lipid were added to obtain surface-functionalized NLC by means of cationic surface charge. Then, 0.01 mg/10 mL of HA was added to the formulation. (Carvajal-Vidal et al., 2019; Sánchez-López et al., 2018).

2.3. Physicochemical parameters

Photon correlation spectroscopy (PCS) was used for measuring zeta average (Z_{av}) and polidispersity index (PI) employing a ZetaSizer Nano ZS (Malvern Instruments, Malvern, UK). Zeta pontetial (ZP) was elucidated by electrophoretic mobility. Prior to measurements, samples were diluted with Milli-Q water 1:10 and analyzed in triplicate at 25 °C. The encapsulation efficiency (EE) was quantified by measuring the non-loaded drug, which was separated from NLC by filtration/centrifugation at 14,000 r.p.m. (Mikro 22 Hettich Zentrifugen, Germany) using an Amicon® Ultra 0.5 centrifugal filter device (Amicon Millipore Corporation, Ireland). Then, the EE was calculated by the difference between the total amount used for the nanoformulation and the free drug, which could be quantified in the filtered fraction, using Eq. (1) (Sánchez-López et al., 2020):

$$EE(\%) = \frac{Total\ amount\ of\ APG - Free\ APG}{Total\ amount\ of\ APG} \times 100 \quad (1)$$

The quantification of APG was performed by a modified reverse-phase high-performance liquid chromatography (RP-HPLC). Briefly, the non-encapsulated drug was quantified using an HPLC Waters 2695 (Waters, Massachusetts, USA) separation module and a Kromasil® C18 column (5 μm, 150 × 4.6 mm), with a mobile phase composed of 2 % acetic acid and methanol, as an aqueous and organic phase respectively. Agradient (from 40 % to 60 % of water phase in 5 min and back in next 5 min) was employed at a flow rate of 0.9 mL·min^{-1}. A diode array detector Waters® 2996 at a wavelength of 300 nm was used to detect APG

and data were processed with Empower 3® Software (Carvajal-Vidal et al., 2019; Romanová et al., 2000).

2.4. Characterization of optimized APG-NLC

2.4.1. Transmission electron microscopy

In order to confirm the spherical morphology of the nanoparticles, transmission electron microscopy (TEM) was used by means of a JEOL 1010 microscope (JEOL USA, Dearborn Road, Peabody, MA 01960, USA). Copper grids were activated with ultraviolet (UV) light, and samples were diluted (1:10) and placed on the grid surface. Prior to TEM analysis, samples were negatively stained with uranyl acetate (2 %) (Sánchez-López et al., 2020).

2.4.2. Interaction studies

Differential scanning calorimetry (DSC) analysis was employed to characterize the thermal behavior of APG-NLC formulations. A DSC 823e System from Mettler-Toledo (Barcelona, Spain) was utilized for this purpose. A pan containing indium (≥99.95 % purity; Fluka, Switzerland) was employed to verify the calibration of the calorimetric system. Throughout the DSC measurements, an empty pan served as a reference. APG-NLC analysis were conducted employing a heating ramp from 25 to 105 °C at a rate of 10 °C/min in an inert nitrogen atmosphere. Data acquired during DSC was analyzed using Mettler STARe V 9.01 dB software (Mettler-Toledo, Barcelona, Spain) (Carvajal-Vidal et al., 2019; Sánchez-López et al., 2020).

X-ray diffraction (XRD) was employed to determine the crystalline state of the samples using the conditions described elsewhere (Carvajal-Vidal et al., 2019).

Fourier transform infrared (FTIR) was used to identify covalent bonds in the samples. FTIR spectra of APG-NLC were acquired using a Thermo Scientific Nicolet iZ10 spectrometer equipped with an ATR diamond crystal and a DTGS detector (Barcelona, Spain) (Esteruelas et al., 2022).

2.5. Stability studies

APG-NLC samples were stored at three different temperatures (4, 25, and 37 °C) for several months. The stability of the formulations was evaluated by analyzing the light backscattering (BS) profiles using a Turbiscan® Lab instrument. A glass measurement cell containing 10 mL of sample was used for each measurement. The BS profiles were acquired at regular intervals of 30 days. The radiation source employed was a pulsed near-infrared light-emitting diode (LED) operating at a wavelength of 880 nm. The BS signal was detected by a detector positioned at a 45° angle from the incident beam. Simultaneously to the BS measurements, values of Z_{av}, PI, ZP, and EE were determined to assess the stability of the APG-NLC formulations (Sánchez-López et al., 2018).

2.6. Biopharmaceutical behavior

The *in vitro* APG release test for APG-NLC was performed using Franz-type diffusion cells (PermeGear Hellertown, USA) with 0.20 cm^2 diffusion area and cellulose dialysis membranes (MWCO 12 kDa). A solution of PBS with 5 % polysorbate 80 and 20 % ethanol under continuous stirring was used as a receptor medium accomplishing sink conditions (ability of the medium to dissolve the expected amount of drug) (Liu et al., 2013). The formulations were compared with free-APG solution. The assay was performed at 32 ± 0.5 °C along 48 h. 150 μL of each formulation were added to the donor compartment by direct contact with the membrane. The drug content of the samples was analyzed by HPLC using the previously described method. The test was performed three times, and the cumulative amount of APG was calculated (Carvajal-Vidal et al., 2019).

2.7. Ocular tolerance

2.7.1. In vitro study: HET-CAM test and HET-CAM TBS

The *in vitro* ocular tolerance of APG-NLC formulations was assessed using the HET-CAM test to evaluate their potential irritation when administered as eye drops. This assay was conducted following the guidelines established by ICCVAM. For each formulation, 300 μL of the test solution was applied to the chorioallantoic membrane of a fertilized chicken egg. Irritation, coagulation, and hemorrhage were monitored during the first 5 min post-application. Both a positive control (0.1 M NaOH) and a negative control (0.9 % NaCl) were included in the study. The ocular irritation index (OII) was calculated by summing the scores assigned to each injury, as defined by the following expression (Eq (2)) (Sánchez-López et al., 2020):

$$OII = \frac{(301 - H)\cdot 5}{300} + \frac{(301 - V)\cdot 7}{300} + \frac{(301 - C)\cdot 9}{300} \quad (2)$$

where H, V and C indicate the time (s) where hemorrhage (H), vasoconstriction (V) and coagulation (C) start to occur. The formulations were categorized based on the following criteria: OII ≤ 0.9 non-irritating; 0.9 < OII ≤ 4.9 weakly irritating; 4.9 < OII ≤ 8.9 moderately irritating; 8.9 < OII ≤ 21 irritating.

Furthermore, at the end of the HET-CAM experiment, in order to quantify the damage of the membrane, trypan blue staining (TBS) was applied. 1000 μL of 0.1 % trypan blue solution were added to the CAM for 1 min. The excess of TBS was removed and the CAM was dissected and extracted with 5 mL of formamide. The absorbance of the extract was then measured spectrophotometrically at a λ_{595nm}. The amount of TBS absorbed was determined using a calibration curve of TBS in formamide (Lagarto et al., 2006).

2.7.2. In vivo ocular tolerance

All experimental procedures were conducted in accordance with the guidelines of the Ethical Committee for Animal Experimentation of the UB and current legislation (Decree 214/97, Gencat). To validate HEM-CAM test results, ocular tolerance of the formulations was assessed *in vivo*. Male New Zealand white rabbits (2.0–2.5 kg, San Bernardo farm, Navarra, Spain) were used in this experiment. A total of 3 rabbits were assigned to each test group. Each rabbit received 50 μL of the respective formulation instilled into the ocular conjunctival sac. A mild massage was applied to ensure proper distribution of the sample within the eye. The eyes were examined for signs of irritation, including corneal opacity and area of involvement, conjunctival hyperemia, chemosis, ocular discharges, and iris abnormalities, at the time of instillation and after 1 h. The contralateral untreated eye served as a negative control. *In vivo* tolerance test scores were assigned based on the observed changes in the anterior segment of the eye, particularly the cornea (turbidity or opacity), iris, and conjunctiva (congestion, chemosis, swelling, and secretion) (Valadares et al., 2021).

2.8. Cellular experiments

2.8.1. Cell culture

Human corneal epithelial cells (HCE-2) (LGC Standards, Barcelona, Spain) were cultured in keratinocyte serum-free growth medium (SFM; Life Technologies, Invitrogen, GIBCO®, Paisley, UK). It was supplemented with bovine pituitary extract 0.05 $mg{\cdot}mL^{-1}$ and epidermal growth factor 5 $ng{\cdot}mL^{-1}$ containing insulin 0.005 $mg{\cdot}mL^{-1}$ and penicillin 100 $U{\cdot}mL^{-1}$ plus streptomycin 100 $mg{\cdot}mL^{-1}$. Cells were grown on a culture flask up to 80 % confluency in a humidified 10 % CO_2 atmosphere at 37 °C (López-Machado et al., 2021).

2.8.2. Cell viability

Cell viability of APG-NLC was assessed using the MTT assay, which measures the reduction of tetrazolium salt by intracellular

dehydrogenases of viable living cells. For this, 100 μL of a cell suspension containing 2 × 10^5 cells/mL was seeded in a 96-well plate and incubated for 48 h at 37 °C in the appropriate complete medium before treatment. Cells were then treated with samples at different concentrations (ranging from 1 × 10^{-3} to 0.1 mg/mL) for 5 or 15 min to simulate real conditions of the cornea. Subsequently, the culture medium was aspirated and replaced with 200 μL of MTT solution (0.25 % w/v in PBS, Sigma-Aldrich Chemical Co., St. Louis, MO, USA). After a 2 h incubation period, the supernatant was replaced with 100 μL of DMSO (99 %, Sigma-Aldrich) to solubilize the formazan product formed by viable cells. Cell viability was determined by measuring the absorbance of the formazan solution at 560 nm using a Modulus® microplate photometer (Turner BioSystems Inc., Sunnyvale, CA, USA). Viability was expressed as a percentage of the untreated control cells (López-Machado et al., 2021; Olivo-Martínez et al., 2023; Folle et al., 2021).

2.8.3. Cellular uptake

To evaluate the internalization of APG-NLC in HCE-2 cells, 1 × 10^5 cell·mL^{-1} HCE-2 were grown in eight-well chamber slider (ibidi®, Gräfelfing, Germany) until 80 % confluence and subsequently incubated with APG-NLC labelled with the fluorescent dye NR at different times (5, 15 and 30 min) at 37 °C. To remove non-internalized NLC, cells were subjected to three washes with PBS. Subsequently, cells were fixed with 4 % paraformaldehyde for 30 min at 25 °C. After fixation, cells were washed three times with PBS to remove unbound paraformaldehyde. The nuclei were stained with DAPI during 10 min. Afterwards, cells were washed using PBS and Alexa Fluor™ 488 conjugated Wheat Germ Agglutinin (WGA) was used to stain cell membranes for 30 min at 25 °C. Cells were washed and finally, mounting solution (PBS) was added for microscopic analysis. Images were acquired using a Leica Thunder Imager DMI8 (Leica Microsystems GmbH, Wetzlar, Germany) with a 63x oil immersion objective lens (López et al., 2020; Gonzalez-Pizarro et al., 2019).

2.9. In vivo efficacy studies

2.9.1. Induction and treatment of dry eye

Twelve male New Zealand white rabbits weighing between 2.0 and 2.5 kg were used for the study. The rabbits were randomly divided into 4 groups: empty NLC, APG-NLC, free APG solution and a commercial solution based on 0.15 % HA. All rabbits were housed at a room temperature of 23 ± 2 °C with relative humidity 75 % ± 10 % and alternating 12 h light–dark cycles.

Both eyes of each rabbit were treated twice-daily with a topical administration of 0.1 % benzalkonium chloride (BAK) for 2 weeks. On day 14, DED was confirmed using the Schirmer test, fluorescein and rose Bengal staining. Treatment commenced after the confirmation of DED, with one eye of each rabbit randomly chosen for twice-daily topical administration of empty NLC, APG-NLC, free APG solution, or a commercial solution (0.15 % HA). After one week of treatment, the Schirmer test, fluorescein staining, and rose Bengal staining were performed again to evaluate the efficacy of the treatments (López-Machado et al., 2021; Xiong et al., 2008).

2.9.1.1. Measurement of aqueous tear production. Tear production was determined using Schirmer test strips. After instilling anesthetic drops containing 1 mg·mL^{-1} tetracaine hydrochloride and 4 mg·mL^{-1} oxybuprocaine hydrochloride, a Schirmer paper strip was placed on the palpebral conjunctiva, positioned near the junction of the middle and outer thirds of the lower eyelid. After 5 min, the extent of wetted paper was measured in millimeters (López-Machado et al., 2021; Xiong et al., 2008).

2.9.1.2. Fluorescein staining on the ocular surface. Fluorescein staining occurs when fluorescein sodium diffuses through disrupted corneal epithelial cell junctions or damaged corneal epithelial cells (Xiong et al., 2008). Corneal fluorescein staining was performed by instilling 2 μL of 1 % fluorescein sodium into the conjunctival sac and allowing it to remain for 2 min. The ocular surface was then examined under a slit lamp microscope equipped with a cobalt blue filter. Images of the ocular surface were captured using a digital camera and scored according to the stained score with 9 indicating maximum score and 0 indicating the minimum (Holzchuh et al., 2011).

2.9.1.3. Rose Bengal staining on the ocular surface. Rose Bengal stains corneal and conjunctival epithelial cells that are not adequately protected by the ocular tear film. It can stain both live and dead cells if they are not protected by an intact mucin layer (Xiong et al., 2008). To assess ocular surface damage, 2 μL of 0.1 % rose Bengal solution were instilled into the conjunctival sac and allowed to remain for 2 min. The ocular surface was then examined under a slit lamp microscope with white light, and images were captured using a digital camera. The degree of staining was assessed using the Van Bijsterveld grading system, and the scores were recorded after 15 s (9: maximum score; 0: minimum) (Xiong et al., 2008).

2.9.2. Anti-inflammatory efficacy

The *in vivo* anti-inflammatory effectiveness of the formulations was evaluated through two studies encompassing inflammation prevention and treatment. Male New Zealand white rabbits (n = 3/group) were used for these experiments as previously described. The activity of APG-NLC was compared with free APG, empty NLC, and 0.9 % NaCl (control group). For the inflammation prevention, 50 μL of each formulation was topically applied to the right eye. After 30 min, a 0.5 % sodium arachidonate (SA) solution dissolved in PBS (inflammatory stimulus) and instilled into the right eye, (left eye served as a control). In the anti-inflammatory treatment study, the inflammatory stimulus was applied 30 min before the application of each formulation. Inflammation was evaluated from the first application up to 210 min following administration, based on the modified ocular tolerance test scoring system (López-Machado et al., 2021; Sánchez-López et al., 2020).

2.10. Statistical analysis

Two-way ANOVA followed by Tukey post hoc test was performed for multi-group comparison. Student's *t*-test was used for two-group comparisons. All the data are presented as the mean ± S.D. Statistical significance was set at $p < 0.05$ by using GraphPad Prism 9.

3. Results

3.1. APG-NLC preparation and optimization

In previous studies, an optimized formulation was obtained (Bonilla-Vidal et al., 2023). In this work, increasing amounts of the cationic lipid DDAB were added to further optimize the formulation (Table 1). The formulation was constituted by Compritol® 888 ATO as the solid lipid component since it provided suitable APG solubility. Compritol® 888 ATO is a well-known excipient used in various administration routes due to its favorable characteristics, including non-polarity, lower

Table 1
Effect of cationic lipid on the physicochemical parameters.

DDAB (%)	Z_{av} ± SD (nm)	PI ± SD	ZP ± SD (mV)
0.025	301.8 ± 2.0	0.186 ± 0.003	−0.8 ± 0.1
0.05	**146.8 ± 0.8**	**0.253 ± 0.003**	**21.2 ± 0.4**
0.06	144.3 ± 2.4	0.326 ± 0.036	27.3 ± 1.0
0.075	150.0 ± 3.8	0.363 ± 0.040	29.3 ± 0.5
0.1	148.2 ± 1.5	0.427 ± 0.018	35.6 ± 0.8
0.3	153.6 ± 1.9	0.407 ± 0.011	54.8 ± 1.6
0.5	147.7 ± 0.3	0.382 ± 0.009	54.4 ± 0.6

cytotoxicity, and its capacity to increase encapsulation efficiency (Aburahma and Badr-Eldin, 2014). Rosehip oil was included as an active ingredient in the formulation to complement the activity of APG with its wound-healing, antioxidant, and anti-inflammatory characteristics (Belkhelladi and Bougrine, 2024; Bhave et al., 2017). The surfactant, Tween® 80, was selected because it is included in official European Medicines Agency (EMA) documents for ocular use at the concentrations employed in this study (Mazet et al, 2020). Additionally, in some cellular models, it has been found to enhance penetration through tight junctions, which could facilitate crossing the human ocular surface epithelial barrier (Khuda et al., 2022; Mantelli et al., 2013).

The optimized formulation was selected based on the physicochemical parameters, with criteria including values of ZP higher than 20 mV and PI lower than 0.3. As a result, the cationic optimized formulation containing 0.05 % of cationic lipid was chosen. Additionally, a small amount of hyaluronic acid (HA) was added. Subsequently, the optimized APG-NLC formulation was obtained.

3.2. Characterization of optimized APG-NLC

TEM analysis revealed that APG-NLC exhibited a predominantly spherical morphology with particle size below 200 nm (specifically, in Fig. 1A APG-NLC size was 166.5 nm), consistent with the results obtained by PCS. Moreover, no particle aggregation phenomena were observed.

DSC was carried out in order to study the crystallinity and melting point variations of the lipid mixtures and APG-NLC. Thermograms (Fig. 1B) showed endothermal peaks of 70.37 °C for lipid mixture, 69.78 °C for lipid mixture-APG and 69.16 °C APG-NLC. The melting point of APG-NLC was slightly lower due to its small size and surfactant presence (Tween® 80) (Bunjes et al., 1996). The peaks moved to slightly lower temperatures when APG was added and the enthalpy was similar between the lipid mixture and lipid mixture-APG being ΔH Lipid mixture = 82.69 Jg^{-1}, ΔH Lipid mixture-APG = 84.03 Jg^{-1} and a smaller enthalpy for the nanoparticles, being ΔH APG-NLC = 54.11 Jg^{-1}. APG melting transition was characterized by an endothermal peak at 365.5 °C (ΔH = 198.5 Jg^{-1}) followed by decomposition, as other authors had also reported (Shakeel et al., 2017).

XRD patterns (Fig. 1C) demonstrated the physicochemical state of APG incorporated into NLC. The presence of intense and sharp peaks for APG and for the solid mixture of lipids indicated a crystalline structure for these components. Notably, the peaks observed for APG were absent in the APG-NLC profile, suggesting that APG was present in a dissolved state within the NLC, forming a molecular dispersion. The crystallinity of the structure of all the components was studied. The lipid mixture showed three peaks in 19.34 (2θ), i.e. $d = 0.46$ nm indicating the most stable form of triacylglycerols, the β form, 21.28 (2θ) i.e. $d = 0.42$ nm and 23.43 (2θ) i.e. $d = 0.38$ nm, which confirmed the existence of the second stable form of triacylglycerols, known as the β' form. The APG-NLC profile showed also the three peaks, which could indicate a good stability of the formulation (Souto et al., 2006; Freitas and Müller, 1999; Zimmermann et al., 2005).

FTIR spectroscopy was employed to investigate the interactions between the drug, the surfactant, and the lipid matrix (Fig. 1D]. The FTIR spectra of APG revealed distinct vibrational bands, including a characteristic peak at 3278 cm^{-1} corresponding to the O–H stretching vibration. The C–H stretching vibration exhibited multiple, smaller peaks at 2800 cm^{-1}. Additionally, the presence of the C-O functional group was indicated by characteristic peaks at 1650 and 1605 cm^{-1}. (Alshehri et al., 2019). There was no evidence of strong bonds between APG and lipid phase and the surfactant. APG peaks were not found in the NLC. These results indicate that APG was encapsulated in the NLC.

3.3. Stability studies

Stability studies were carried out analyzing the BS profiles of each sample at different temperatures. BS provides information of destabilization mechanisms in the media, such as sedimentation, creaming, or aggregation (Bonilla-Vidal et al., 2023). In this way, BS profiles of APG-NLC were studied at 4, 25 and 37 °C (Fig. 2A-C). APG-NLC was stable at 4 °C for a period of 25 months, while at 25 °C the stability was 1 month. The physicochemical parameters were kept constant at 4 °C for all the

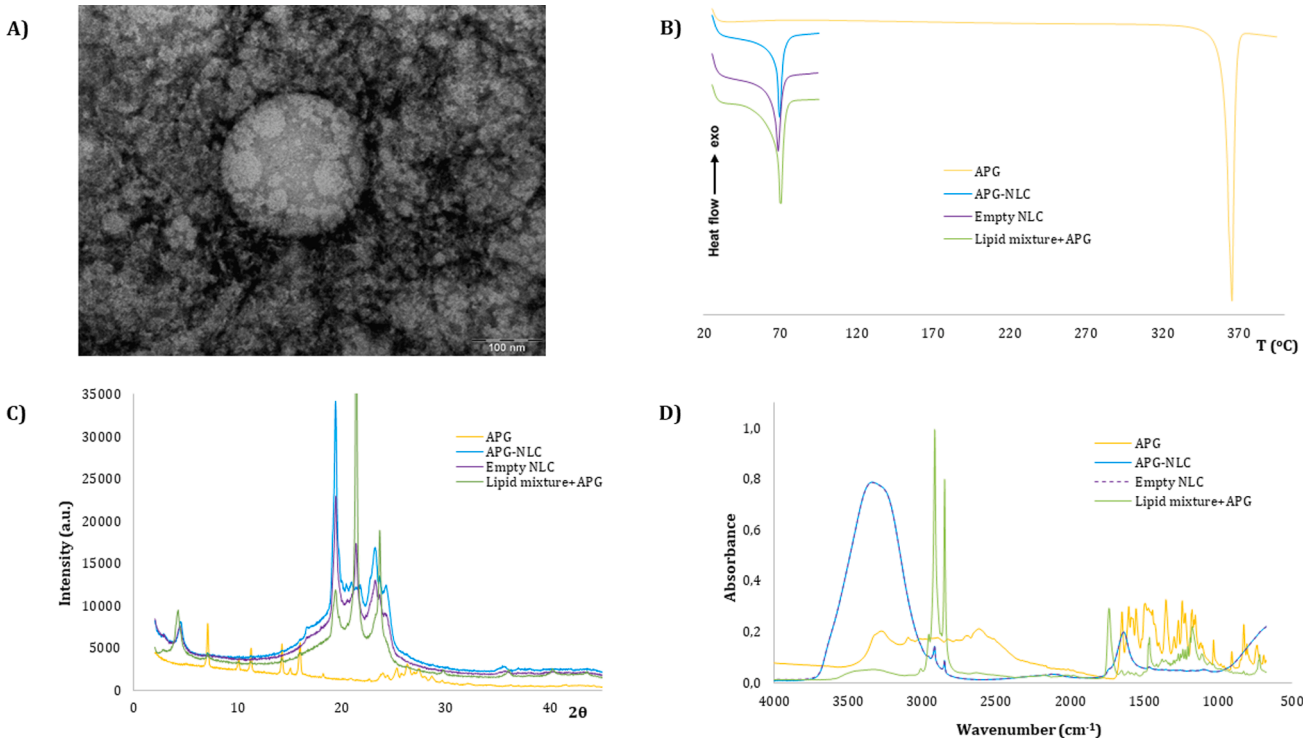

Fig. 1. Characterization of optimized APG-NLC and their components. (A) TEM image (scale bar 100 nm), (B) DSC curves, (C) XRD patterns, (D) FTIR analysis.

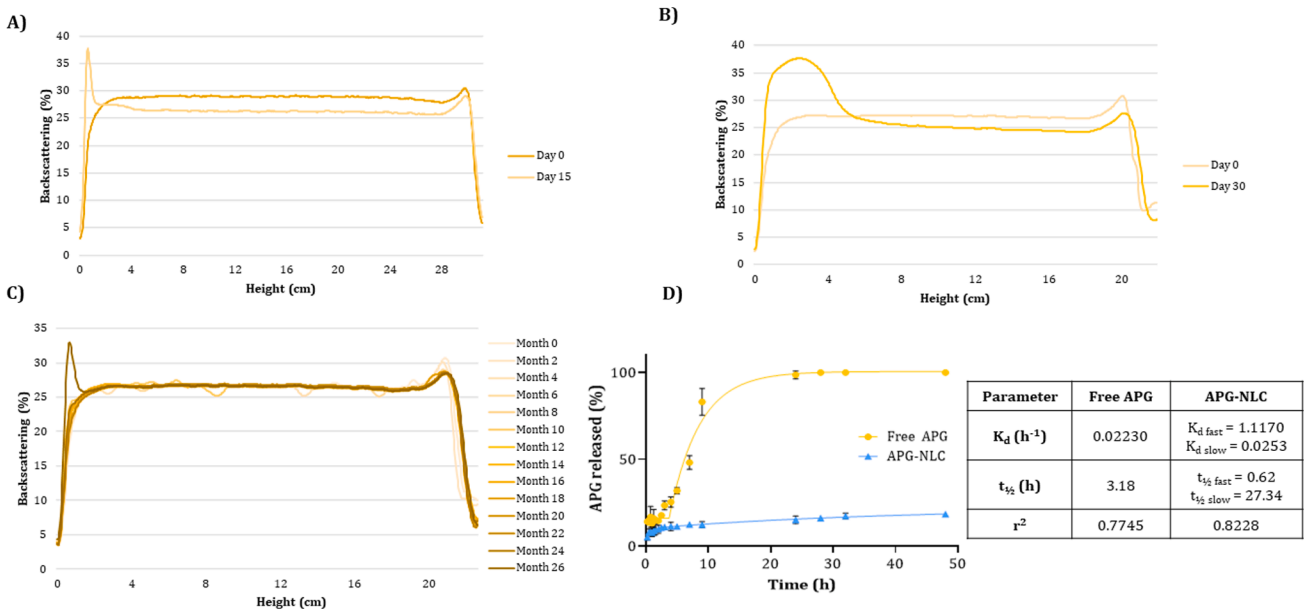

Parameter	Free APG	APG-NLC
K_d (h^{-1})	0.02230	$K_{d\ fast}$ = 1.1170 $K_{d\ slow}$ = 0.0253
$t_{½}$ (h)	3.18	$t_{½\ fast}$ = 0.62 $t_{½\ slow}$ = 27.34
r^2	0.7745	0.8228

Fig. 2. Characterization of APG-NLC. Backscattering profiles of APG-NLC stored at (A) 37 °C, (B) 25 °C, and (C) 4 °C. (D) *In vitro* release profile of APG-NLC vs free APG carried out for 48 h and adjustment to a two-phase decay and Plateau followed by one phase decay model respectively.

study, being the most suitable storage temperature.

3.4. Biopharmaceutical behavior

The *in vitro* release profile of APG from the NLC exhibited a biphasic drug release pattern, characteristic of prolonged drug delivery systems. A two-phase decay model provided the best fit for APG-NLC release (Fig. 2). An initial burst release of APG was observed during the first 2 h, followed by a sustained release phase that lasted until the end of the experiment. In contrast, free APG exhibited a rapid diffusion, reaching 100 % release within 24 h, while the APG-NLC formulation released only approximately 30 % during the same time period. The dissociation constant (K_d) values for APG-NLC were significantly higher in fast release phase compared to those of free APG (1.1170 vs 0.02230 h), suggesting a rapid initial release, followed by a slower one (Liu et al., 2013). Moreover, half-life results ($t_{1/2}$) showed that initially there was a burst release during the fast phase of the formulation, and then it was followed by a slow phase, in which it had a sustained and lower release, with a $t_{1/2}$ value of 9.14 h.

3.5. Ocular tolerance

Ocular tolerance was studied *in vitro* using the HET-CAM test and *in vivo* using the Draize test (Fig. 3A-D). The HET-CAM test results demonstrated that the positive control (1 M NaOH, 18.75 ± 1.05) induced severe hemorrhage, intensifying over a 5-minute period. This characterization classifies the solution as a severe irritant. In contrast, application of the negative control (0.9 % NaCl, 0.07 ± 0.01) and both the loaded and empty formulations to the chorioallantoic membrane did not elicit any signs of irritation, leading to their classification as non-irritant substances (0.07 ± 0.01 and 0.07 ± 0.01 respectively). Otherwise, free APG caused a fast vasoconstriction, being classified as a severe irritant (14.86 ± 0.30). Moreover, TBS quantitative results supported the results of the HET-CAM test, where APG-NLC were non-irritant while free APG resulted irritant (0.06 ± 0.04 and 0.18 ± 0.01 respectively).

However, as a single *in vitro* test is insufficient to accurately assess ocular tolerance in a living organism, ocular tolerance Draize tests were conducted to further evaluate the formulations. The tests were carried out with free APG, empty NLC, and APG-NLC. In this sense, none of the developed NLC were irritant *in vivo* or *in vitro*, while the free APG

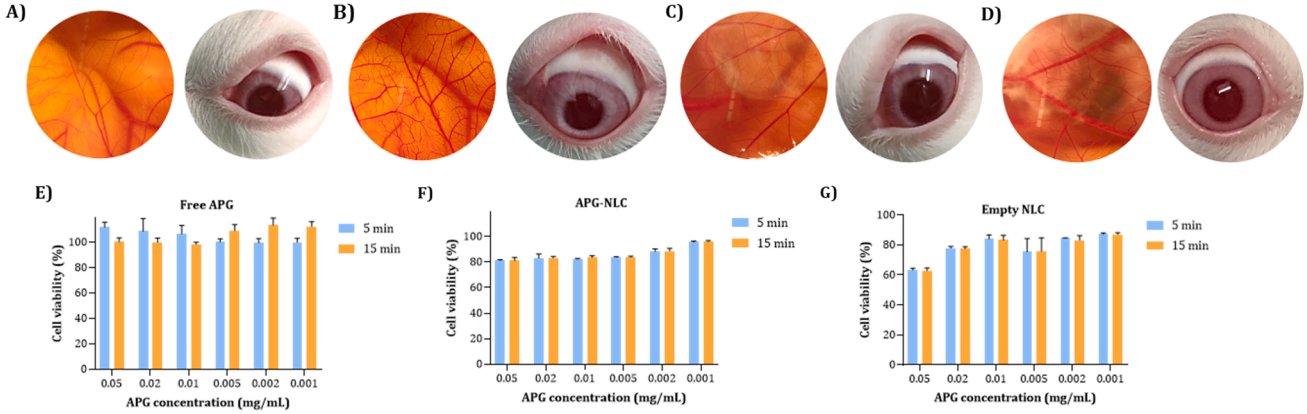

Fig. 3. Ocular tolerance. *In vitro* and *in vivo* irritation assay. (A) Negative control, NaCl 0.9 %, (B) Free APG, (C) APG-NLC, and (D) Empty NLC. (E) Scores obtained on the HET-CAM and *in vivo* ocular tolerance. (F-H) Effect of (F) free APG, (G) APG-NLC and (H) empty NLC on the viability of HCE-2 cells at 5 and 15 min. 100 % cell viability corresponds to the average of MTT reduction values of untreated cells.

resulted irritant *in vitro* (14.86 ± 0.30) and non-irritant *in vivo* (2.00 ± 1.00) but caused an initial discomfort. These results confirmed the non-irritant potential of APG loaded lipid nanoparticles, meanwhile the free APG can induce some discomfort.

3.6. Cellular experiments

3.6.1. Cell viability in corneal cells

Cell viability of several concentrations of free APG, APG-NLC, and empty NLC (without APG) were evaluated on HCE-2 cells. The HCE-2 cell line was selected to analyze the compatibility of the formulations on corneal cells after topical administration. Samples were incubated for various time points to simulate the real conditions of contact between the formulation and the cornea in humans (Mofidfar et al., 2021). For this reason, cell viability was tested incubating for 5 and 15 min. According to ISO 10993–5, percentages of cell viability above 80 % are considered non-cytotoxic; within 80 – 60 % weak; 60 – 40 % moderate and below 40 % strongly cytotoxic, respectively (López-García et al., 2014). Results showed that after 5- and 15-min incubation, free APG did not cause relevant cytotoxic effects (≥80 % viability). Free APG did not show any effects on cell viability at any of the concentrations tested or incubation times (Fig. 3F). APG-NLC after 5- and 15- min incubation showed suitable cell viability in all the assessed concentrations (Fig. 3G). Similarly, empty NLC resulted in suitable cell viability for 5- and 15- min incubation from 0.02 to 0.001 mg·mL^{-1} (Fig. 3H). The most concentrated dilution of empty NLC showed weak toxicity at both times. However, it can be observed that APG-NLC were safe (high cell viability) in all the studied concentrations.

3.6.2. Cellular uptake

Following incubation at different time points, fluorescent NLC were visualized using fluorescence microscopy. The nucleus was stained with DAPI, and the cell membrane was stained with Alexa Fluor™ 488-WGA to facilitate better bio-localization of the NLC. In the merged images, APG-NLC were observed inside the cells, indicating that the particles were able to penetrate without altering the morphology of the corneal

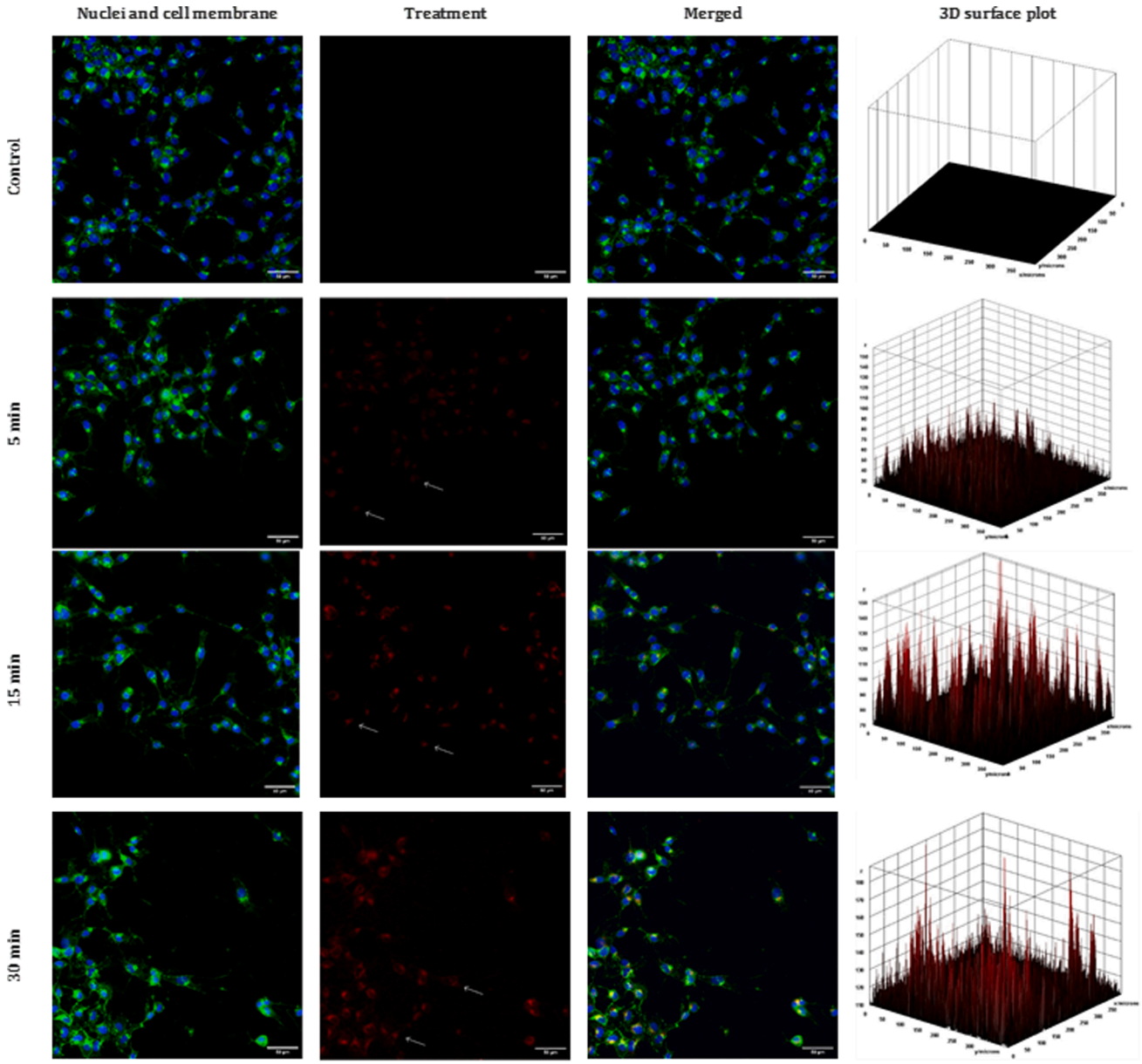

Fig. 4. Cellular uptake of APG-NLC in HCE-2 at different incubation time (5, 15, or 30 min). White arrows highlight samples localization. Surface plot is shown as relative fluorescence intensity per cell in 3D coordinates.

cells (Fig. 4). It is noteworthy that toxic substances, such as benzalkonium chloride, can induce morphological changes in the cell membrane, such as vacuolization of corneal cells Kinnunen et al, 2014. Moreover, the fluorescence signal had increased along with the incubation time. Furthermore, after 30 min incubation of APG-NLC displayed higher intensity than cells incubated 5 or 15 min. No fluorescence was observed in the control cells (Fig. 4).

3.7. Induction and treatment of DED

In order to evaluate the potential to treat DED using APG-NLC, Schirmer test, fluorescein and rose Bengal assessments were performed to measure the effects of empty NLC, free APG and commercial solution based on 0.15 % of HA as a moisturizing agent.

3.7.1. Schirmer test

To evaluate the improvement on tear flow caused by the developed NLC in a DED model, Schirmer's test was employed. A marked decrease in aqueous tear secretion was observed after applying BAK for 2 weeks. Fig. 5A shows the differences between each experimental group. Empty NLC and APG-NLC were able to increase the tear flow obtaining statistically significant differences against DED control, $p < 0.01$ and $p < 0.0001$ respectively. Otherwise, free APG and the 0.15 % HA solution did not improve tear flow. APG-NLC showed statistically significant differences between all the groups: $p < 0.05$ against empty NLC, and $p < 0.0001$ against free APG and 0.15 % HA solution. Empty NLC showed statistically significant differences between free APG group ($p < 0.05$). Interestingly, APG-NLC was the only treatment that showed statistically significant differences compared to 0.15 % HA solution ($p < 0.0001$).

3.7.2. Fluorescein staining on the ocular surface

Fluorescein staining is an effective method for evaluating the state of the ocular surface. It results from fluorescein uptake, which is caused by the disruption of corneal epithelial cell–cell junctions or damaged corneal epithelial cells (Begley et al., 2019; Srinivas and Rao, 2023). Fig. 5B shows the differences between each experimental group. There were statistically significant differences between all the groups against dry eye control. However, the two treatments that provided the best improvement on the ocular corneal surface were empty NLC and APG-NLC ($p < 0.001$, 0.67 ± 0.58 and 1.00 ± 1.00 respectively). Moreover, free APG solution and the 0.15 % HA solution presented higher staining (2.33 ± 0.58 and 3.00 ± 1.15 respectively), indicating a diminished capacity to restore the corneal surface (Fig. 6).

3.7.3. Rose Bengal staining on the ocular surface

Rose Bengal is a valuable tool for assessing tear film integrity. It selectively stains corneal and conjunctival epithelial cells that are exposed due to compromised preocular tear film protection. Its ability to stain both live and dead cells, provided the mucin layer is disrupted, enables it to detect various degrees of tear film dysfunction (Xiong et al., 2008). As can be observed in Fig. 5C, there were statistically significant differences between dry eye control and empty NLC and APG-NLC staining (5.08 ± 1.78, 1.67 ± 1.15 and 1.67 ± 1.15 respectively). The results showed that only NLC were able to restore the disrupted tear film. Moreover, HA 0.15 % solution (4.67 ± 1.15) did not show significant differences against the control, indicating that it did not exert significant tear film restoring capacity (Fig. 7).

3.8. Anti-inflammatory efficacy

Anti-inflammatory efficacy was assessed in New Zealand rabbits to elucidate the capacity of the developed APG-NLC to treat and/or prevent ocular inflammation.

Firstly, the *in vivo* inflammation treatment was assessed. Fig. 8A revealed that the degree of inflammation was significantly reduced after the first 30 min post-administration of APG-NLC. Free APG were able to rapidly treat inflammation. Moreover, empty NLC exerted anti-inflammatory activity after 90 min of instillation. Comparing APG-NLC with empty NLC, it can be observed that APG-NLC had significantly higher anti-inflammatory effects than empty NLC after 2 h post-application, probably due to APG prolonged release.

The *in vivo* inflammation prevention test revealed significant differences in the severity of inflammation between APG formulations and the control at all time points evaluated (Fig. 8B). However, APG-NLC-treated eyes exhibited a more rapid reduction in corneal edema compared to free APG. This finding can be attributed to the rapid tear clearance of free APG and the lipid components of the nanoparticles that may result in a prolonged drug residence time within the cornea. APG-NLC demonstrated superior inflammation-relieving effects compared to the control over time. Otherwise, empty NLC also showed an anti-inflammatory effect *in vivo*. Initially, the effect was similar to the APG-NLC activity, but after 90 min of treatment a significant anti-inflammatory effect produced by APG can be observed since significant differences between empty NLC and APG-NLC were obtained (Strugała et al., 2016).

Thus, APG-NLC exhibited a preventive effect on inflammatory processes caused by the sustained release of APG and the synergic activity of

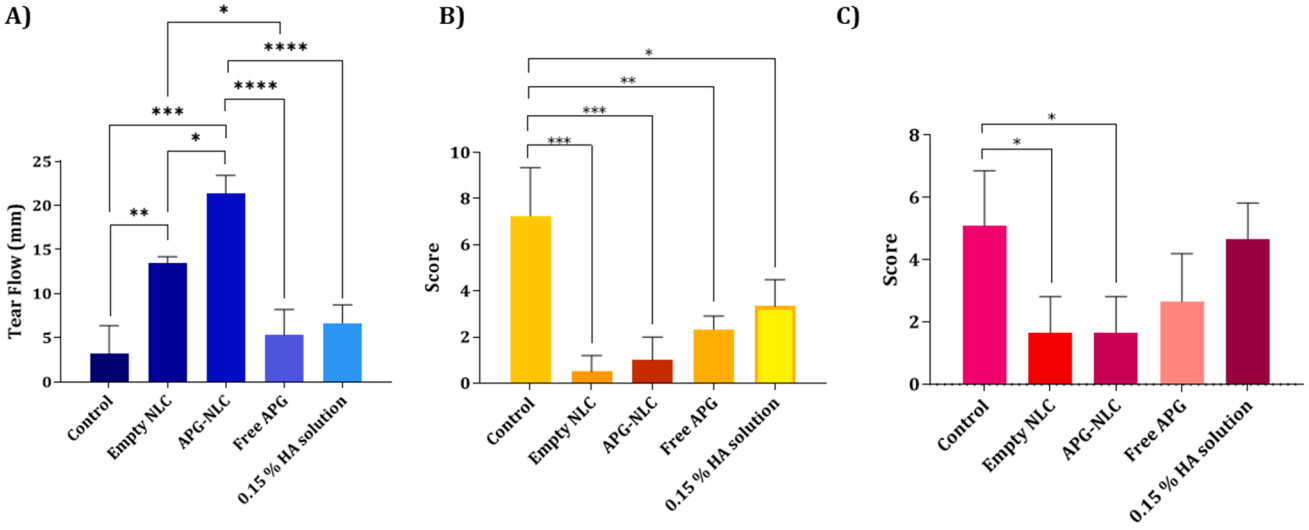

Fig. 5. DED results with statistically significant differences (* $p < 0.05$, ** $p < 0.01$, *** $p < 0.001$; **** $p < 0.0001$). (A) Schirmer test, (B) Fluorescein staining, (C) Rose Bengal staining.

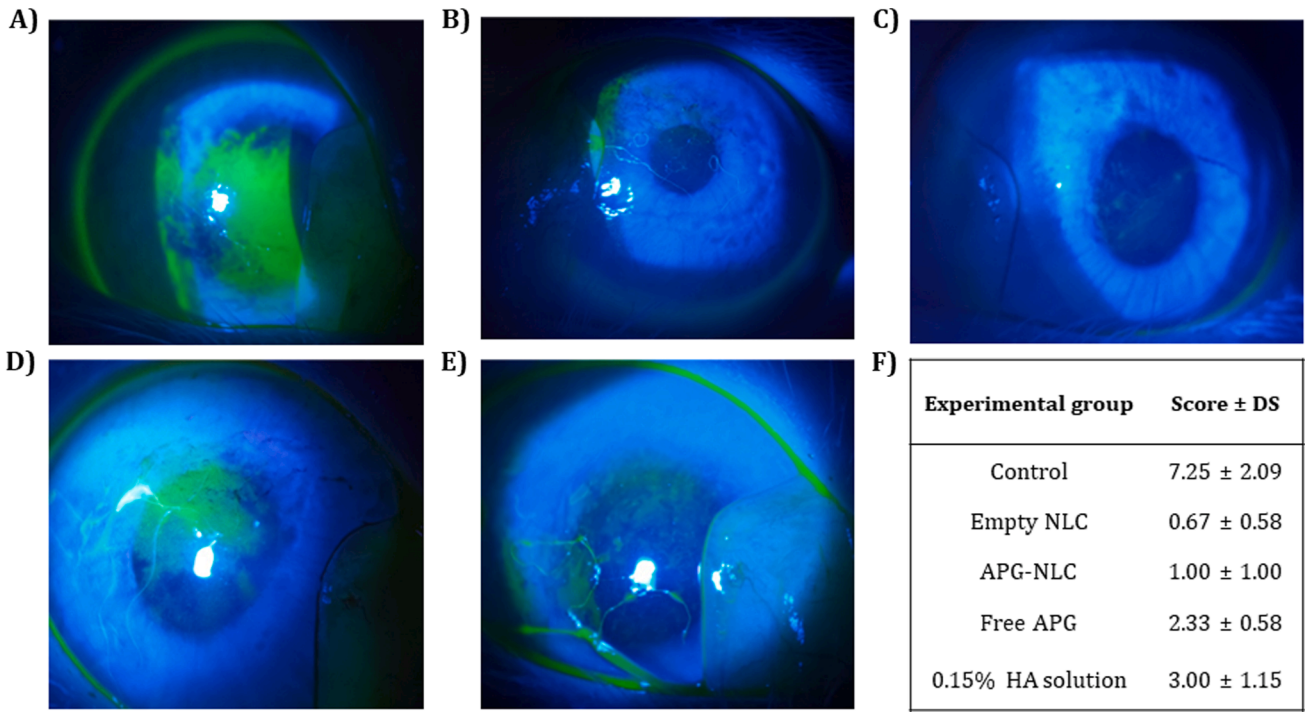

Experimental group	Score ± DS
Control	7.25 ± 2.09
Empty NLC	0.67 ± 0.58
APG-NLC	1.00 ± 1.00
Free APG	2.33 ± 0.58
0.15% HA solution	3.00 ± 1.15

Fig. 6. Fluorescein staining test. (A) Control. (B) Empty NLC (C) APG-NLC. (D) 0.15 HA % solution. (E) Free APG (F) Scores obtained on the fluorescein staining test.

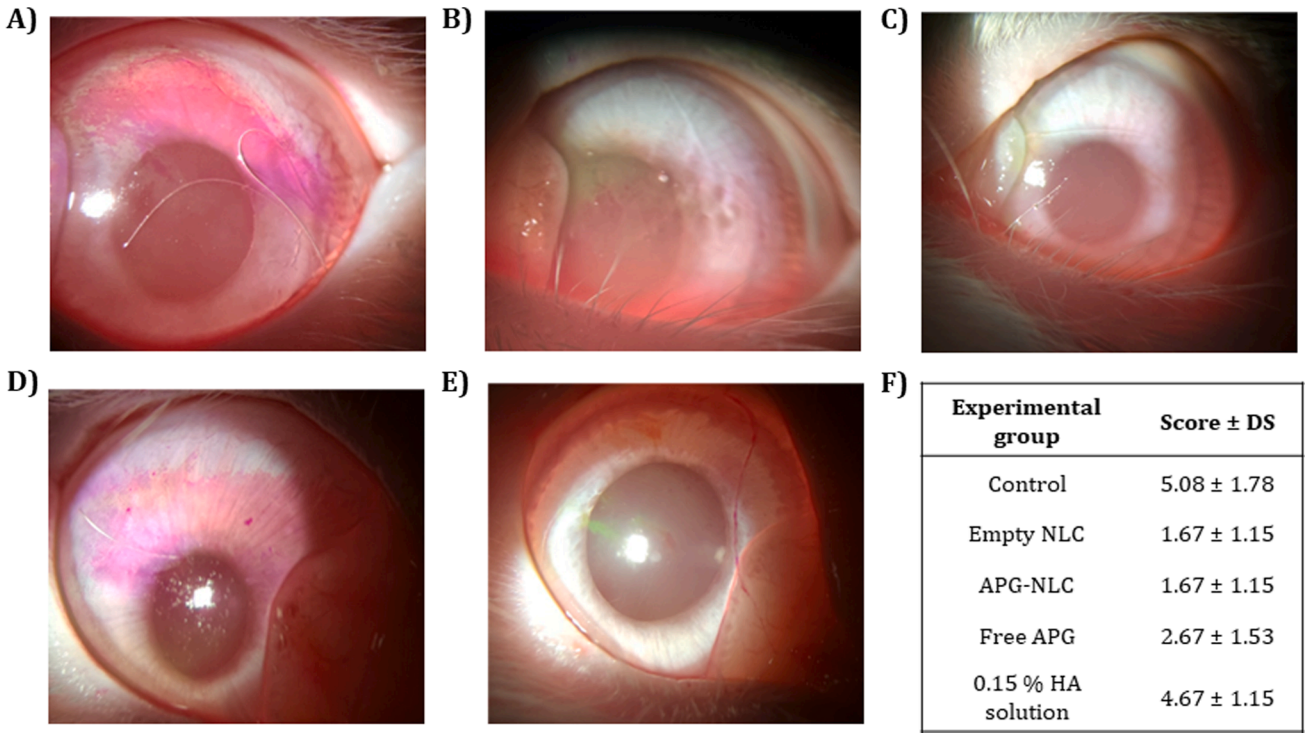

Experimental group	Score ± DS
Control	5.08 ± 1.78
Empty NLC	1.67 ± 1.15
APG-NLC	1.67 ± 1.15
Free APG	2.67 ± 1.53
0.15 % HA solution	4.67 ± 1.15

Fig. 7. Rose Bengal staining test. (A) Control. (B) Empty NLC. (C) APG-NLC. (D) 0.15 % HA solution. (E) Free APG. (F) Scores obtained on the rose Bengal staining test.

the vehicle, which may contribute towards an initial anti-inflammatory effect.

Hence, it can be confirmed that APG-NLC possess ocular anti-inflammatory activity, both for prevention and inflammation treatment. Furthermore, the vehicle also showed anti-inflammatory properties, which could be attributed to the rosehip oil (Winther et al., 2016).

4. Discussion

In this study, a new formulation was developed loading APG into a cationic rosehip-based NLC coated with HA. APG-NLC was prepared using the hot high-pressure homogenization method, which is widely used for lipid nanoparticle fabrication. The high temperature facilitates greater size reduction due to lower inner-phase viscosity. Furthermore,

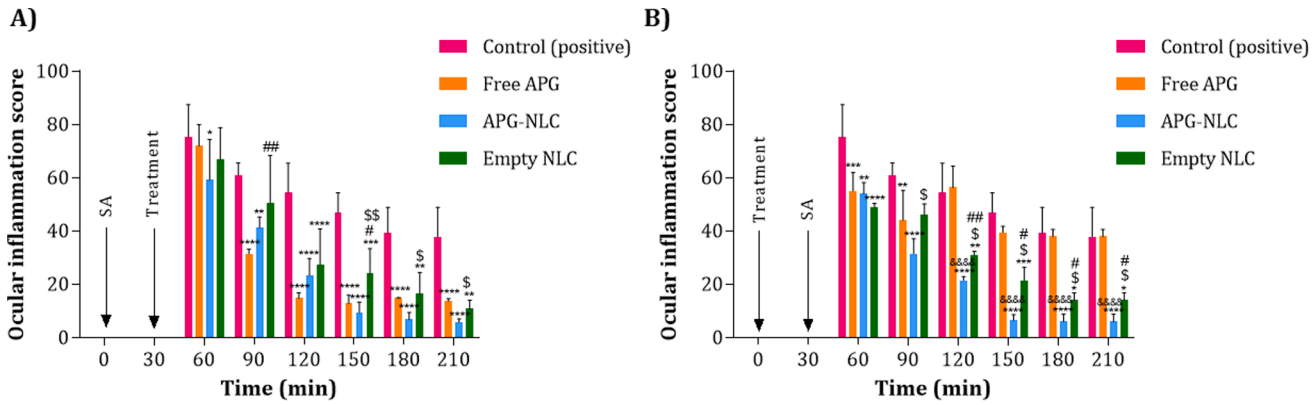

	Experimental groups	60 min	90 min	120 min	150 min	180 min	210 min
Inflammation treatment	Control vs Free APG	ns	****	****	****	****	****
	Control vs APG-NLC	*	**	****	****	****	****
	Control vs Empty NLC	ns	ns	****	***	**	**
	Free APG vs APG-NLC	ns	ns	ns	ns	ns	ns
	Free APG vs Empty NLC	ns	##	ns	#	ns	ns
	APG-NLC vs Empty NLC	ns	ns	ns	$$	$	$
Inflammation prevention	Control vs Free APG	***	**	ns	ns	ns	ns
	Control vs APG-NLC	**	****	****	****	****	****
	Control vs Empty NLC	****	ns	**	***	*	*
	Free APG vs APG-NLC	ns	ns	&&&&	&&&&	&&&&	&&&&
	Free APG vs Empty NLC	ns	ns	##	#	#	#
	APG-NLC vs Empty NLC	ns	$	$	$	$	$

Fig. 8. Comparison of ocular anti-inflammatory efficacy of free APG, APG-NLC, and empty NLC. SA (sodium arachidonate) was used as inflammatory stimuli. (A) Inflammation treatment, (B) inflammation prevention. Values are expressed as mean ± SD; ns: non-significant, *p < 0.05, **p < 0.01, ***p < 0.005, and ****p < 0.001 significantly lower than the inflammatory effect induced by SA; $p < 0.05 and $$p < 0.05 significantly lower effect of APG-NLC than the inflammatory effect induced by empty NLC; &&&&p < 0.0001 significantly lower effect of APG-NLC than the corresponding free drug; #p < 0.05 and ##p < 0.01 significantly lower effect of empty NLC than the corresponding free drug.

this method offers several advantages such as ease of scale-up, absence of organic solvents, and shorter production times (Vinchhi et al., 2021; Khairnar et al., 2022). Sterile fabrication is facilitated by equipment that can be sterilized using steam, and manufacturing can be conducted in an aseptic environment in a laminar airflow unit (Khairnar et al., 2022). Additionally, sterile filtration, autoclaving, ionizing radiation, and non-ionizing radiation can be used in the final formulation for sterilization, with gamma radiation being one of the most commonly used methods (Bernal-Chávez et al., 2021; Youshia et al., 2021).

The cationic lipid DDAB was used in order to increase the ocular retention time on the ocular surface and mucoadhesion due to electrostatic interactions between the negatively charged ocular surface and the nanocarrier. Cationic carriers have shown to effectively penetrate through the negatively charged pores of the corneal epithelium, making them an interesting tool to obtain an efficient drug delivery (Abruzzo et al., 2021; Vedadghavami et al., 2020). Furthermore, the formulation was improved with the addition of HA, which possesses a relatively high viscosity, improving tear film stability and reducing the washout from the ocular surface. Additionally, it promotes epithelial wound healing, which could work in synergy with the liquid lipid (rosehip oil) (Johnson et al., 2006).

In order to optimize the concentration of DDAB, increasing amounts of it were added to the previously optimized formulation (Bonilla-Vidal et al., 2023). The results showed that the Z_{av} was similar from 0.05 to 0.5 %, while the PI and the ZP increased when higher amounts were added. For this reason, the selected concentration was 0.05 %, providing a PI below 0.3, indicating an homogeneous distribution of the nanoparticles, and a ZP around + 20 mV, which contributed to overcome the attractive forces between particles, achieving suitable stability of the colloidal system (Bonilla et al., 2022).

Interaction studies showed that the addition of APG to the lipid matrix resulted in an increase in the amorphous structure of the lipids, suggesting that APG was internalized in the lipid matrix (Ojo et al., 2020). Further analysis using FTIR confirmed that no covalent bonds were formed between APG and the lipid matrix, implying that the interaction between them was primarily mediated by hydrogen bonds and hydrophobic forces. This interaction facilitated the entrapment of APG within the NLC and promoted its release from the particles (Huang et al., 2020). Additionally, XRD studies indicated that APG-NLC exhibited good stability over an extended period due to the presence of the most stable forms of triacylglycerols in Compritol® 888 ATO, namely, the β and β' phases (Souto et al., 2006; Freitas and Müller, 1999; Zimmermann et al., 2005). These findings align with the stability studies, which demonstrated that the formulation remained stable at 4 °C for 25 months. However, at the end of the 25-month period, the electrostatic forces between the APG-NLC may have begun to weaken, leading to aggregation and sedimentation, as observed in the BS profile. In comparison to the previous studies in which the negatively charged formulation (without DDAB nor HA), the stability at 4 °C endured for 11 months (Bonilla-Vidal et al., 2023). The main difference between both formulations was the addition of the cationic lipid, which has a chemical structure and physicochemical properties of a surfactant. The addition of a co-surfactant into the formulation may contribute to stabilize the emulsion droplets during homogenization and upon polymorphic transition during storage, as other studies confirmed (Salminen et al., 2014).

Furthermore, APG-NLC showed a slow *in vitro* release profile, whereas the APG solution exhibited a rapid diffusion. The fitted model for APG-NLC was a two-phase association, due to the fact that the formulation demonstrated a dual release profile, offering an initial fast release followed by a sustained release, where approximately a 20 % of APG was liberated into the receptor medium. This two-phase release pattern could be attributed to the formulation ability to encapsulate APG

within the NLC while also facilitating its gradual diffusion into the medium. Compared to our previous studies, this formulation showed a faster release in the initial phase with a higher rate constant ($K_{d\ fast}$ = 0.2662 vs 1.1170 h^{-1} of the negatively and positively charged formulation respectively), and a more sustained release in the slow phase, with a much lower constant ($K_{d\ slow}$ = 0.0662 vs 0.0253 h^{-1} of the negatively and positively charged formulation respectively) (Bonilla-Vidal et al., 2023). These differences could be related to its modified surface with DDAB and HA. It has been documented that HA surface modification can restrict water diffusion into the carrier matrix which subsequently slows down the drug release process (Huang et al., 2017).

In order to demonstrate the safety of APG-NLC at the ocular level, *in vitro* experiments were carried out. HCE-2 cells were used to evaluate the cytocompatibility of the APG-NLC in a corneal cell line. The results showed that free APG was safe at all the tested concentrations (0.050–0.001 mg·mL^{-1}) which indicates that APG was non-toxic in this corneal epithelial cell line. Similarly, empty NLC resulted non-toxic in the majority of the assessed concentrations. This may be due to its positive charge, which produces a higher electrostatic attraction between negatively charged cell surfaces, leading to increase in oxidative stress and reactive oxygen species (ROS) (Yang et al., 2021). Furthermore, lipid components of NLC may possess affinity for cell membranes, which facilitates the interaction between them (Zhang et al., 2014). However, APG-NLC was safe in all the tested concentrations (except for the higher ones where it was slightly toxic). This effect could be related with the protective activity of APG on these cells. Some authors reported that APG was able to protect corneal cells from excessive superoxide radicals and hydrogen peroxide (Bigagli et al., 2017). Moreover, in a DED study, APG showed to protect the cells due to its anti-inflammatory activity (Liu et al., 2019). Otherwise, the internalization of the NLC was performed to evaluate their capacity to interact with HCE-2 cells by labelling APG-NLC with the fluorescent NR. In this study, it has been demonstrated that APG-NLC quickly interacted with corneal cells in the first 5 min of incubation. Furthermore, with increasing incubation time, the NLC increased its accumulation inside the cells. No changes in the morphology of the HCE-2 cells were observed, which confirmed its *in vitro* safety in comparison to toxic substances such as BAK (Kinnunen et al., 2014).

To evaluate the ocular safety of the formulation, an *in vitro* HET-CAM test was conducted. The HET-CAM test allows observation of vascular responses due to the acute effects of the test substance on the small blood vessels and soft tissue proteins of the CAM. These responses are similar to those produced by the substance in the rabbit eye, owing to the similar vascular and inflammatory framework of the eye conjunctival tissue (Valadares et al., 2021; Abdelkader et al., 2012). Other methods used to evaluate ocular tolerability, such as the bovine corneal opacity and permeability (BCOP) assay or the isolated chicken eye assay, are employed to study the opacity and permeability of the cornea (Lebrun et al., 2021). Results demonstrated that APG was irritating when directly applied to the CAM. However, both the empty and loaded NLC were non-irritating, indicating that the encapsulation strategy effectively mitigates the irritation potential of APG. These results were also confirmed by the HET-CAM TBS, a quantitative assay based on the ability of trypan blue to stain damaged or dead cells (Vinardell and García, 2000). *In vivo* testing within the eye offers advantages for studying chemical damage due to the presence of physiological response and repair mechanisms in living tissue. However, severe damage from the chemicals themselves can impede these repair processes. While *in vitro* methods are used to assess acute effects from a single application, they fail to consider the reversibility of these lesions (Valadares et al., 2021; Cazedey et al., 2009; Budai et al., 2021). The tolerance ocular test incorporates a post-treatment period to allow for healing, providing a more complete picture. While the tear layer can act as a barrier and influence the absorption of water-soluble chemicals, it can also wash away the test substance, reducing its efficacy. The HET-CAM test, while useful for assessing conjunctival damage due to its similarity to human ocular tissue, may not fully capture corneal irritation, which is a key focus of the *in vivo* tolerance test (Budai et al., 2021). For this reason, to confirm the safety of the formulations, an *in vivo* ocular tolerance assessment was carried out. The results showed that free APG caused an initial discomfort in the rabbits, but it did not cause irritation or redness on the eye. Furthermore, results confirmed that neither APG-NLC nor empty NLC caused any irritation, which demonstrates that the formulations were safe for ocular administration.

The potential activity of APG-NLC against DED was demonstrated through an *in vivo* assay based on the induction of DED by administering BAK twice daily for two weeks, followed by one-week treatment. BAK is a commonly used eye drop preservative with inherent detergent properties that destabilize the tear film's lipid layer. This leads to increased evaporation of the aqueous tear layer and decreased tear film break-up time, leaving the ocular surface vulnerable to dryness and irritation. Additionally, BAK directly targets the corneal epithelium, the outermost layer of the cornea, exhibiting a dose-dependent cytotoxic effect. BAK effects can also trigger an inflammatory response characterized by increased expression of various inflammatory markers such as interleukins and TNF-α, as well as infiltration of immune cells into the conjunctiva (Rosin and Bell, 2013; Lin et al., 2011). Chronic exposure to BAK can lead to a heightened inflammatory state, which promotes the recruitment of fibroblasts and subsequent fibrosis of the subconjunctival tissue (Rosin and Bell, 2013; Clouzeau et al., 2012). The four treatment groups studied in this work were APG-NLC, empty NLC to elucidate the effect of the lipid matrix, free APG to observe its therapeutic potential, and a commercial artificial tear based on HA as a commonly used first line treatment of DED. Three different evaluation assays were conducted to determine both the induction of DED and the efficacy of the treatments: i) Schirmer test, ii) fluorescein staining, iii) rose bengal staining. The Schirmer test constitutes a simple diagnostic procedure used to assess tear production. The test relies on the principle of capillary action, which allows the water content of tears to migrate along the length of a filter paper strip. The rate of migration along the strip corresponds to the tear production rate (Nr and Y, 2020). The results of the Schirmer test showed that APG-NLC were the treatment that attained the best score, followed by the empty NLC, indicating that both were able to restore the tear secretion of the animals. These results reveal the potential of the composition of the nanoformulations to restore tear flow *in vivo*. APG-NLC presented a significantly better score than all the other groups, probably due to APG encapsulation. APG possess anti-inflammatory properties, improving DED associated inflammation (Kashyap et al., 2018). In this study, free APG was not able to restore the tear flow which may be attributed to the high clearance of APG when it was administered as eyedrops (Lanier et al., 2021). Furthermore, regarding tear volume, the commercial solution (0.15 % HA solution) did not show significant differences against the control either due to the short-treatment period (5-days) or to HA short-lifespan at the ocular level (Semp et al., 2023).

In order to evaluate the improvement of the ocular surface, fluorescein and rose bengal staining were used. Fluorescein penetrates poorly into the lipid layer of the corneal epithelium. However, fluorescein readily binds to areas where the cell-to-cell junctions of the corneal epithelium are disrupted. This property makes it an effective tool for detecting corneal abrasions, ulcers, and other injuries (Srinivas and Rao, 2023). In this study, all the tested formulations showed a lower score than dry eye control, which means that all were able to improve the corneal epithelium. Specifically, APG-NLC and empty NLC were the treatments with higher statistical differences between dry eye control (*** $p < 0.001$). It is well known that rosehip oil possesses wound healing properties when applied to the skin, but there is no information about its ocular use (Lei et al., 2019). It has been described that rosehip oil influence on skin wound healing is hypothesized to be mediated by promoting the phenotypic transition of macrophages from the M1 to the M2 state. M1 macrophages are characterized by their pro-inflammatory activity, while M2 macrophages contribute to extracellular matrix

regeneration and the resolution of inflammation (Belkhelladi and Bougrine, 2024). Other actions such as its capacity to increase the collagen III content in wound tissue, and inhibit epithelial-mesenchymal transition during wound healing to improve scarring has been also described in dermal applications (Criollo-Mendoza et al., 2023). In this study, the lipid matrix was able to improve the corneal injuries produced by DED, which could be related to its wound healing, anti-inflammatory and antioxidant properties (Strugała et al., 2016; Lei et al., 2019). In the same manner, when this active matrix was loaded with APG, an improvement of the corneal injuries was observed, which could be also attributed to APG anti-inflammatory and anti-oxidant properties (Kashyap et al., 2018). On the other hand, rose bengal is a dye that stains any part of the ocular surface that is not adequately covered by tear film, particularly areas lacking mucin (Srinivas and Rao, 2023; Doughty, 2013). In this study, only the nanoformulations were able to restore the tear film. This fact could be related to the lipids that are used to prepare the NLC, which usually had occlusive and moisturizing effects (Bonilla et al., 2022). The 0.15 % HA solution and free APG did not show statistically significant differences, may be due to the fast clearance that artificial tears and small molecules undergo in the ocular surface (Weng et al., 2018). In comparison to other drug delivery systems, NLC exhibit high potential for the treatment of DED. Composed of lipid assemblies, NLC exhibit high mucoadhesive properties towards corneal epithelial cells, which may extend precorneal retention time and sustained release of encapsulated therapeutics. In previous studies it has been described that NLC adhere to the glycocalyx, a protective layer on the corneal epithelium, facilitating gradual release of their lipid components into the tear film (Niamprem et al., 2019). Lipids would then integrate within the tear film lipid layer, enhancing its stability and reducing tear evaporation (Niamprem et al., 2019). Furthermore, other *in vivo* studies demonstrated that NLC exhibited prolonged precorneal film formation, promoting tear film stability under desiccated conditions and protecting corneal epithelial cells from damage. These findings suggest that NLC possess properties similar to a biomimetic tear film, offering potential as a therapeutic strategy for tear replacement and replenishment in DED treatment (Niamprem et al., 2019).

It is well-established that inflammation is part of DED pathology and it is triggered by the activation of innate immune components within ocular surface cells, a decrease in tear film stability, and an elevated tear osmolarity. For this reason, anti-inflammatory eye drops may be used but they possess associated side effects (Perez et al., 2020; Yagci and Gurdal, 2014). Therefore, *in vivo* experiments were carried out to explore the anti-inflammatory activity of APG-NLC, in which treatment and prevention of the inflammation by using SA as an inflammatory stimulus were performed. In the treatment assay, it was observed that free APG had a great anti-inflammatory response 1 h after application. APG is a flavone with a well-known anti-inflammatory activity, which decreases inflammatory markers (Ginwala et al., 2019). To date, there have been no reports indicating that APG acts as an anti-inflammatory molecule when administered ocularly. Only a few studies have demonstrated the *in vitro* capacity of APG to reduce certain inflammatory markers. For instance, it has been described that APG alleviated TNF-α-induced apoptosis in retinal ganglion cells (Fu et al., 2014). Furthermore, one of the plants that contains APG, chamomile, has shown several properties when applied ocularly (Bigagli et al., 2017). Eye drops containing chamomile and Euphrasia, showed to protect corneal epithelial cells exhibiting wound healing activity, strong antioxidant activity, and anti-inflammatory properties by decreasing COX-2, IL-1β, iNOS expression. Otherwise, empty NLC also exerted an anti-inflammatory activity 1.5 h after instillation. As mentioned above, rosehip oil has been reported to possess anti-inflammatory activity, then the reduction of the inflammation exerted by SA could be reduced. APG-NLC resulted very effective in the treatment of inflammation because of their reduction of swelling since the first 30 min of instillation. This effect could be related to the combined effect of all the components in the nanoparticles, in which the release of APG from the NLC possessed an initial burst and a posterior sustained release, increasing its anti-inflammatory properties, and the rosehip oil present in the lipid matrix could also contribute to the activity exerted. On the other hand, the *in vivo* experiment about the prevention of the inflammation highlighted the potential of APG-NLC to prevent the inflammation caused by DED. In this assessment, the free APG showed its properties at the beginning of the experiment, which could be related to its fast clearance from the ocular surface, being not able to exert its full activity. The empty formulation also showed a fast action, mainly related to the presence of rosehip oil. Finally, APG-NLC was the most effective treatment, probably due to the NLC composition. Firstly, its cationic charge and HA improved its mucoadhesion to the ocular surface, followed by the action of the lipid matrix, mainly the rosehip oil, and the initial burst release of APG. Then, it could be observed that when APG was released, the ocular inflammation score was progressively reduced, almost reaching the minimum. Therefore, after topical application, the synergy of all the components in APG-NLC produced a suitable anti-inflammatory response.

These results showed the ability of the lipid nanoparticles to revert the signs of DED. Empty NLC and APG-NLC were able to improve all the studied parameters of DED. These results could be due to the novel composition of the nanoparticles. The addition of the rosehip oil grants anti-inflammatory and antioxidant properties to NLC (Kiralan and Yildirim, 2019; Lin et al., 2017). Because of this fact, empty NLC showed interesting properties against DED. The addition of APG improved the tear secretion on the Schirmer test, probably due to its encapsulation in NLC conferring improved anti-inflammatory properties against DED symptomatology.

5. Conclusions

In summary, a novel nanotechnological approach has been developed for the effective management of DED and its associated ocular complications. This approach involves encapsulating APG within cationic NLC coated with HA, resulting in a nanosystem with suitable physical stability and sustained APG release. Extensive *in vitro* and *in vivo* assessments confirm the biocompatibility of the developed NLC, with no adverse effects on ocular tissues and demonstrated uptake by corneal cells. Additionally, APG-NLC exhibit enhanced therapeutic efficacy in DED and ocular inflammation animal models. Empty NLC also ameliorate DED signs, but the addition of APG to NLC improved tear flow and anti-inflammatory capacity. Hence, APG-NLC may represent a promising system for the treatment and prevention of DED.

CRediT authorship contribution statement

L. Bonilla-Vidal: Writing – original draft, Methodology, Investigation, Formal analysis. **M. Espina:** Writing – review & editing, Methodology, Investigation, Formal analysis. **M.L. García:** Writing – review & editing, Methodology, Funding acquisition, Conceptualization. **L. Baldomà:** Writing – review & editing, Methodology, Investigation, Funding acquisition. **J. Badia:** Writing – review & editing, Methodology, Investigation, Funding acquisition. **J.A. González:** Investigation, Conceptualization. **L.M. Delgado:** Methodology, Investigation. **A. Gliszczyńska:** Writing – review & editing, Supervision, Investigation. **E. B. Souto:** Writing – review & editing, Investigation, Formal analysis. **E. Sánchez-López:** Writing – review & editing, Supervision, Methodology, Investigation, Funding acquisition, Formal analysis.

Declaration of competing interest

Research data and results obtained are protected under patent (PCT/EP2024/052923). LB, ME, MLG and ESL hold the intellectual property of the mentioned patent.

Data availability

No data was used for the research described in the article.

Acknowledgements

This research was supported by the Spanish Ministry of Science and Innovation (PID2021-122187NB-C32) and a Llavors project (LLAV 0004). EBS acknowledges FCT—Fundação para a Ciência e a Tecnologia, I.P., in the scope of the project UIDP/04378/2020 and UIDB/04378/2020 of the Research Unit on Applied Molecular Biosciences—UCIBIO and the project LA/P/0140/ 2020 of the Associate Laboratory Institute for Health and Bioeconomy—i4HB. E.S.-L. acknowledges the support of Grants for the Requalification of the Spanish University System.

References

Abdelkader, H., Ismail, S., Hussein, A., Wu, Z., Al-Kassas, R., Alany, R.G., 2012. Conjunctival and corneal tolerability assessment of ocular naltrexone niosomes and their ingredients on the hen's egg chorioallantoic membrane and excised bovine cornea models. Int. J. Pharm. 432 (1–2), 1–10.

Abruzzo, A., Giordani, B., Miti, A., Vitali, B., Zuccheri, G., Cerchiara, T., et al., 2021. Mucoadhesive and mucopenetrating chitosan nanoparticles for glycopeptide antibiotic administration. Int. J. Pharm. 606, 120874.

Aburahma, M.H., Badr-Eldin, S.M., 2014. Compritol 888 ATO: a multifunctional lipid excipient in drug delivery systems and nanopharmaceuticals. Expert Opin. Drug Deliv. 11 (12), 1865–1883.

Agarwal, P., Craig, J.P., Rupenthal, I.D., 2021. Formulation considerations for the management of dry eye disease. Pharmaceutics. 13 (2), 207.

Alshehri, S.M., Shakeel, F., Ibrahim, M.A., Elzayat, E.M., Altamimi, M., Mohsin, K., et al., 2019. Dissolution and bioavailability improvement of bioactive apigenin using solid dispersions prepared by different techniques. Saudi Pharm J. 27 (2), 264–273.

Baiula, M., Spampinato, S., 2021. Experimental pharmacotherapy for dry eye disease: a review. J. Exp. Pharmacol. 13, 345–358.

Battaglia, L., Serpe, L., Foglietta, F., Muntoni, E., Gallarate, M., Del Pozo, R.A., et al., 2016. Application of lipid nanoparticles to ocular drug delivery. Expert Opin. Drug Deliv. 13 (12), 1743–1757.

Begley, C., Caffery, B., Chalmers, R., Situ, P., Simpson, T., Nelson, J.D., 2019. Review and analysis of grading scales for ocular surface staining. Ocul. Surf. 17 (2), 208–220.

Belkhelladi, M., Bougrine, A., 2024. Rosehip extract and wound healing: A review. J. Cosmet. Dermatol. 23 (1), 62–67.

Bernal-Chávez, S.A., Del Prado-Audelo, M.L., Caballero-Florán, I.H., Giraldo-Gomez, D. M., Figueroa-Gonzalez, G., Reyes-Hernandez, O.D., et al., 2021. Insights into terminal sterilization processes of nanoparticles for biomedical applications. Molecules 26 (7).

Bhave, A., Schulzova, V., Chmelarova, H., Mrnka, L., Hajslova, J., 2017. Assessment of rosehips based on the content of their biologically active compounds. J. Food Drug Anal. 25 (3), 681–690.

Bigagli, E., Cinci, L., D'Ambrosio, M., Luceri, C., 2017. Pharmacological activities of an eye drop containing Matricaria chamomilla and Euphrasia officinalis extracts in UVB-induced oxidative stress and inflammation of human corneal cells. J. Photochem. Photobiol. B Biol. 173, 618–625.

Bonilla, L., Espina, M., Severino, P., Cano, A., Ettcheto, M., Camins, A., et al., 2022. Lipid nanoparticles for the posterior eye segment. Pharmaceutics. 14 (1), 90.

Bonilla-Vidal, L., Świtalska, M., Espina, M., Wietrzyk, J., García, M.L., Souto, E.B., et al., 2023. Dually active apigenin-loaded nanostructured lipid carriers for cancer treatment. Int. J. Nanomed. 18, 6979–6997.

Budai, P., Kormos, É., Buda, I., Somody, G., Lehel, J., 2021. Comparative evaluation of HET-CAM and ICE methods for objective assessment of ocular irritation caused by selected pesticide products. Toxicol Vitr. 74, 105150.

Bunjes, H., Westesen, K., Koch, M.H.J., 1996. Crystallization tendency and polymorphic transitions in triglyceride nanoparticles. Int. J. Pharm. 129 (1–2), 159–173.

Carvajal-Vidal, P., Fábrega, M.J., Espina, M., Calpena, A.C., García, M.L., 2019. Development of Halobetasol-loaded nanostructured lipid carrier for dermal administration: Optimization, physicochemical and biopharmaceutical behavior, and therapeutic efficacy. Nanomedicine Nanotechnology, Biol Med. 20, 102026.

Cazedey, E.C.L., Carvalho, F.C., Fiorentino, F.A.M., Gremião, M.P.D., Salgado, H.R.N., 2009. Corrositex®, BCOP and HET-CAM as alternative methods to animal experimentation. Brazilian J Pharm Sci. 45 (4), 759–766.

Clouzeau, C., Godefroy, D., Riancho, L., Rostène, W., Baudouin, C., Brignole-Baudouin, F., 2012. Hyperosmolarity potentiates toxic effects of benzalkonium chloride on conjunctival epithelial cells in vitro. Mol. Vis. 18, 863.

Craig, J.P., Nichols, K.K., Akpek, E.K., Caffery, B., Dua, H.S., Joo, C.K., et al., 2017. TFOS DEWS II definition and classification report. Ocul. Surf. 15 (3), 276–283.

Criollo-Mendoza, M.S., Contreras-Angulo, L.A., Leyva-López, N., Gutiérrez-Grijalva, E.P., Jiménez-Ortega, L.A., Heredia, J.B., 2023. Wound healing properties of natural products: mechanisms of action. Molecules 28 (2), 598.

De Paiva, C.S., 2017. Effects of aging in dry eye. Int. Ophthalmol. Clin. 57 (2), 64.

Doughty, M.J., 2013. Rose bengal staining as an assessment of ocular surface damage and recovery in dry eye disease—A review. Contact Lens Anterior Eye. 36 (6), 272–280.

Esteruelas, G., Halbaut, L., García-Torra, V., Espina, M., Cano, A., Ettcheto, M., et al., 2022. Development and optimization of Riluzole-loaded biodegradable nanoparticles incorporated in a mucoadhesive in situ gel for the posterior eye segment. Int. J. Pharm. 612, 121379.

Fangueiro, J.F., Calpena, A.C., Clares, B., Andreani, T., Egea, M.A., Veiga, F.J., et al., 2016. Biopharmaceutical evaluation of epigallocatechin gallate-loaded cationic lipid nanoparticles (EGCG-LNs): In vivo, in vitro and ex vivo studies. Int. J. Pharm. 502 (1–2), 161–169.

Folle, C., Marqués, A.M., Díaz-Garrido, N., Espina, M., Sánchez-López, E., Badia, J., et al., 2021. Thymol-loaded PLGA nanoparticles: an efficient approach for acne treatment. J Nanobiotechnology. 19 (1), 359.

Freitas, C., Müller, R.H., 1999. Correlation between long-term stability of solid lipid nanoparticles (SLN) and crystallinity of the lipid phase. Eur. J. Pharm. Biopharm. 47 (2), 125–132.

Fu, M.-S., Zhu, B.-J., Luo, D.-W., 2014. Apigenin prevents TNF-α induced apoptosis of primary rat retinal ganglion cells. Cell. Mol. Biol. 60 (4), 37–42.

Ginwala, R., Bhavsar, R., Chigbu, D.G.I., Jain, P., Khan, Z.K., 2019. Potential role of flavonoids in treating chronic inflammatory diseases with a special focus on the anti-inflammatory activity of apigenin. Antioxidants. 8 (2), 35.

Gonzalez-Pizarro, R., Parrotta, G., Vera, R., Sánchez-López, E., Galindo, R., Kjeldsen, F., et al., 2019. Ocular penetration of fluorometholone-loaded PEG-PLGA nanoparticles functionalized with cell-penetrating peptides. Nanomedicine 14 (23), 3089–3104.

Holzchuh, R., Villa Albers, M.B., Osaki, T.H., Igami, T.Z., Santo, R.M., Kara-Jose, N., et al., 2011. Two-year outcome of partial lacrimal punctal occlusion in the management of dry eye related to Sjögren syndrome. Curr. Eye Res. 36 (6), 507–512.

Huang, D., Chen, Y.S., Rupenthal, I.D., 2017. Hyaluronic acid coated albumin nanoparticles for targeted peptide delivery to the retina. Mol. Pharm. 14 (2), 533–545.

Huang, L., Gao, H., Wang, Z., Zhong, Y., Hao, L., Du, Z., 2021. Combination nanotherapeutics for dry eye disease treatment in a rabbit model. Int. J. Nanomed. 16, 3631.

Huang, Z., Ma, C., Wu, M., Li, X., Lu, C., Zhang, X., et al., 2020. Exploring the drug-lipid interaction of weak-hydrophobic drug loaded solid lipid nanoparticles by isothermal titration calorimetry. J Nanoparticle Res. 22 (1), 1–14.

Johnson, M.E., Murphy, P.J., Boulton, M., 2006. Effectiveness of sodium hyaluronate eyedrops in the treatment of dry eye. Graefe's Arch Clin Exp Ophthalmol. 244 (1), 109–112.

Kashyap, D., Sharma, A., Tuli, H.S., Sak, K., Garg, V.K., Buttar, H.S. et al., 2018. Apigenin: A natural bioactive flavone-type molecule with promising therapeutic function. vol. 48, Journal of Functional Foods. Elsevier Ltd, pp. 457–471.

Kelly, J.D.S., Nichols, K., Sheppard, J.D., Nichols, K.K., 2023. Dry eye disease associated with Meibomian gland dysfunction: focus on tear film characteristics and the therapeutic landscape. Ophthalmol Ther. 12 (3), 1397–1418.

Khairnar, S.V., Pagare, P., Thakre, A., Nambiar, A.R., Junnuthula, V., Abraham, M.C., et al., 2022. Review on the scale-up methods for the preparation of solid lipid nanoparticles. Pharmaceutics. 14 (9), 1886.

Khuda, S.E., Nguyen, A.V., Sharma, G.M., Alam, M.S., Balan, K.V., Williams, K.M., 2022. Effects of emulsifiers on an in vitro model of intestinal epithelial tight junctions and the transport of food allergens. Mol. Nutr. Food Res. 66 (4), e2100576.

Kinnunen, K., Kauppinen, A., Piippo, N., Koistinen, A., Toropainen, E., Kaarniranta, K., 2014. Cationorm shows good tolerability on human HCE-2 corneal epithelial cell cultures. Exp Eye Res. 120, 82–89.

Kiralan, M., Yildirim, G., 2019. Rosehip (Rosa canina L.) Oil. Fruit Oils Chem Funct. 803–814.

Kumari, S., Dandamudi, M., Rani, S., Behaeghel, E., Behl, G., Kent, D., et al., 2021. Dexamethasone-loaded nanostructured lipid carriers for the treatment of dry eye disease. Pharmaceutics. 13 (6), 905.

Lagarto, A., Vega, R., Guerra, I., González, R., 2006. In vitro quantitative determination of ophthalmic irritancy by the chorioallantoic membrane test with trypan blue staining as alternative to eye irritation test. Toxicol. In Vitro 20 (5), 699–702.

Lanier, O.L., Manfre, M.G., Bailey, C., Liu, Z., Sparks, Z., Kulkarni, S., et al., 2021. Review of approaches for increasing ophthalmic bioavailability for eye drop formulations. AAPS PharmSciTech 22 (3), 1–16.

Lebrun, S., Nguyen, L., Chavez, S., Chan, R., Le, D., Nguyen, M., et al., 2021. Same-chemical comparison of nonanimal eye irritation test methods: Bovine corneal opacity and permeability, EpiOcular™, isolated chicken eye, ocular Irritection®, OptiSafe™, and short time exposure. Toxicol Vitr. 72, 105070.

Lei, Z., Cao, Z., Yang, Z., Ao, M., Jin, W., Yu, L., 2019. Rosehip oil promotes excisional wound healing by accelerating the phenotypic transition of macrophages. Planta Med. 85 (7), 563–569.

Lin, Z., Liu, X., Zhou, T., Wang, Y., Bai, L., He, H., et al., 2011. A mouse dry eye model induced by topical administration of benzalkonium chloride. Mol. Vis. 17, 264.

Lin, T.K., Zhong, L., Santiago, J.L., 2017. Anti-inflammatory and skin barrier repair effects of topical application of some plant oils. Int. J. Mol. Sci. 19 (1), 70.

Liu, P., De Wulf, O., Laru, J., Heikkilä, T., Van Veen, B., Kiesvaara, J., et al., 2013. Dissolution studies of poorly soluble drug nanosuspensions in non-sink conditions. AAPS PharmSciTech 14 (2), 748.

Liu, L., Wei, D., Xu, H., Liu, C., 2019. Apigenin ameliorates ocular surface lesions in a rat model of dry eye disease. Eur. J. Inflamm. 17.

López, E.S., Machado, A.L.L., Vidal, L.B., González-Pizarro, R., Silva, A.D., Souto, E.B., 2020. Lipid nanoparticles as carriers for the treatment of neurodegeneration associated with Alzheimer's disease and glaucoma: present and future challenges. Curr. Pharm. Des. 26 (12), 1235–1250.

López-García, J., Lehocký, M., Humpolíček, P., Sáha, P., 2014. HaCaT keratinocytes response on antimicrobial atelocollagen substrates: extent of cytotoxicity, cell viability and proliferation. J Funct Biomater. 5 (2), 57.

López-Machado, A., Díaz-Garrido, N., Cano, A., Espina, M., Badia, J., Baldomà, L., et al., 2021. Development of lactoferrin-loaded liposomes for the management of dry eye disease and ocular inflammation. Pharmaceutics. 13 (10), 1698.
Mantelli, F., Mauris, J., Argüeso, P., 2013. The ocular surface epithelial barrier and other mechanisms of mucosal protection: from allergy to infectious diseases. Curr. Opin. Allergy Clin. Immunol. 13 (5), 563–568.
Mazet, R., Yaméogo, J.B.G., Wouessidjewe, D., Choisnard, L., Gèze, A., 2020. Recent Advances in the Design of Topical Ophthalmic Delivery Systems in the Treatment of Ocular Surface Inflammation and Their Biopharmaceutical Evaluation. Pharmaceutics. 12 (6), 570.
Mofidfar, M., Abdi, B., Ahadian, S., Mostafavi, E., Desai, T.A., Abbasi, F., et al., 2021. Drug delivery to the anterior segment of the eye: A review of current and future treatment strategies. Int. J. Pharm. 607, 120924.
Niamprem, P., Milla, T.J., Schuett, B.S., Srinivas, S.P., Tiyaboonchai, W., 2019. Interatcion of nanostructured lipid carriers with human meibum. Int J Appl Pharm. 11 (3), 35–42.
Niamprem, P., Teapavarapruk, P., Srinivas, S.P., Tiyaboonchai, W., 2019. Impact of nanostructured lipid carriers as an artificial tear film in a rabbit evaporative dry eye model. Cornea 38 (4), 485–491.
Nr, B., Y, R., 2020. Schirmer test. Encycl Ophthalmol. 1–2.
Ojo, A.T., Ma, C., Lee, P.I., 2020. Elucidating the effect of crystallization on drug release from amorphous solid dispersions in soluble and insoluble carriers. Int. J. Pharm. 591, 120005.
Olivo-Martínez, Y., Bosch, M., Badia, J., Baldomà, L., 2023. Modulation of the intestinal barrier integrity and repair by microbiota extracellular vesicles through the differential regulation of trefoil factor 3 in LS174T goblet cells. Nutrients 15 (11), 2437.
Peng, W., Jiang, X., Zhu, L., Li, X., Zhou, Q., Wu, Y.J.M., et al., 2022. Cyclosporine A (0.05%) ophthalmic gel in the treatment of dry eye disease: A multicenter, randomized, double-masked, phase III, COSMO trial. Drug Des. Devel. Ther. 16, 3183–3194.
Perez, V.L., Stern, M.E., Pflugfelder, S.C., 2020. Inflammatory basis for dry eye disease flares. Exp. Eye Res. 201, 108294.
Periman, L.M., Mah, F.S., Karpecki, P.M., 2020. A review of the mechanism of action of Cyclosporine A: the role of Cyclosporine A in dry eye disease and recent formulation developments. Clin. Ophthalmol. 14, 4200.
Romanová, D., Grančai, D., Józová, B., Božek, P., Vachálková, A., 2000. Determination of apigenin in rat plasma by high-performance liquid chromatography. J. Chromatogr. A 870 (1–2), 463–467.
Rosin, L.M., Bell, N.P., 2013. Preservative toxicity in glaucoma medication: clinical evaluation of benzalkonium chloride-free 0.5% timolol eye drops. Clin. Ophthalmol. 7, 2135.
Salminen, H., Helgason, T., Aulbach, S., Kristinsson, B., Kristbergsson, K., Weiss, J., 2014. Influence of co-surfactants on crystallization and stability of solid lipid nanoparticles. J. Colloid Interface Sci. 426, 256–263.
Sánchez-López, E., Ettcheto, M., Egea, M.A., Espina, M., Cano, A., Calpena, A.C., et al., 2018. Memantine loaded PLGA PEGylated nanoparticles for Alzheimer's disease: In vitro and in vivo characterization. J Nanobiotechnology. 16 (1), 1–16.
Sánchez-López, E., Esteruelas, G., Ortiz, A., Espina, M., Prat, J., Muñoz, M., et al., 2020. Dexibuprofen biodegradable nanoparticles: one step closer towards a better ocular interaction study. Nanomaterials 10 (4).
Semp, D.A., Beeson, D., Sheppard, A.L., Dutta, D., Wolffsohn, J.S., 2023. Artificial tears: a systematic review. Clin. Optom. 15, 27.
Shakeel, F., Alshehri, S., Ibrahim, M.A., Elzayat, E.M., Altamimi, M.A., Mohsin, K., et al., 2017. Solubility and thermodynamic parameters of apigenin in different neat solvents at different temperatures. J. Mol. Liq. 234, 73–80.
Silva, A.M., Martins-Gomes, C., Fangueiro, J.F., Andreani, T., Souto, E.B., 2019. Comparison of antiproliferative effect of epigallocatechin gallate when loaded into cationic solid lipid nanoparticles against different cell lines. Pharm. Dev. Technol. 24 (10), 1243–1249.
Souto, E.B., Mehnert, W., Müller, R.H., 2006. Polymorphic behaviour of Compritol888 ATO as bulk lipid and as SLN and NLC. J. Microencapsul. 23 (4), 417–433.
Srinivas, S.P., Rao, S.K., 2023. Ocular surface staining: Current concepts and techniques. Indian J. Ophthalmol. 71 (4), 1089.
Strugała, P., Gładkowski, W., Kucharska, A.Z., Sokół-Łetowska, A., Gabrielska, J., 2016. Antioxidant activity and anti-inflammatory effect of fruit extracts from blackcurrant, chokeberry, hawthorn, and rosehip, and their mixture with linseed oil on a model lipid membrane. Eur. J. Lipid Sci. Technol. 118 (3), 461–474.
Valadares, M.C., de Oliveira, G.A.R., de Ávila, R.I., da Silva, A.C.G., 2021. Strategy combining nonanimal methods for ocular toxicity evaluation. Methods Mol. Biol. 2240, 175–195.
Vedadghavami, A., Zhang, C., Bajpayee, A.G., 2020. Overcoming negatively charged tissue barriers: Drug delivery using cationic peptides and proteins. Nano Today 34, 100898.
Vinardell, M., García, L., 2000. The quantitive chlorioallantoic membrane test using trypan blue stain to predict the eye irritancy of liquid scintillation cocktails. Toxicol Vitr. 14 (6), 551–555.
Vinchhi, P., Patel, J.K., Patel, M.M., 2021. High-pressure homogenization techniques for nanoparticles. Emerg Technol Nanoparticle Manuf. 263–285.
Wang, M., Firrman, J., Liu, L.S., Yam, K., 2019. A review on flavonoid apigenin: Dietary intake, ADME, antimicrobial effects, and interactions with human gut microbiota. Biomed Res. Int. 7010467.
Wei, J., Mu, J., Tang, Y., Qin, D., Duan, J., Wu, A., 2023. Next-generation nanomaterials: advancing ocular anti-inflammatory drug therapy. J Nanobiotechnology. 21 (1), 1–60.
Weng, Y.-H., Ma, X.-W., Che, J., Li, C., Liu, J., Chen, S.-Z., et al., 2018. Nanomicelle-assisted targeted ocular delivery with enhanced antiinflammatory efficacy in vivo. Adv. Sci. 5 (1), 1700455.
Winther, K., Sophie, A., Hansen, V., Campbell-Tofte, J., 2016. Bioactive ingredients of rose hips (Rosa canina L) with special reference to antioxidative and anti-inflammatory properties: in vitro studies. Bot Targets Ther. 6, 23.
Xiong, C., Chen, D., Liu, J., Liu, B., Li, N., Zhou, Y., et al., 2008. A rabbit dry eye model induced by topical medication of a preservative benzalkonium chloride. Invest. Ophthalmol. Vis. Sci. 49 (5), 1850–1856.
Yagci, A., Gurdal, C., 2014. The role and treatment of inflammation in dry eye disease. Int. Ophthalmol. 34 (6), 1291–1301.
Yang, W., Wang, L., Mettenbrink, E.M., Deangelis, P.L., Wilhelm, S., 2021. Nanoparticle toxicology. Annu. Rev. Pharmacol. Toxicol. 61, 269–289.
Youshia, J., Kamel, A.O., El Shamy, A., Mansour, S., 2021. Gamma sterilization and in vivo evaluation of cationic nanostructured lipid carriers as potential ocular delivery systems for antiglaucoma drugs. Eur. J. Pharm. Sci. 163.
Zhang, W., Li, X., Ye, T., Chen, F., Yu, S., Chen, J., et al., 2014. Nanostructured lipid carrier surface modified with Eudragit RS 100 and its potential ophthalmic functions. Int. J. Nanomed. 9, 4315.
Zhang, Y., Yang, Y., Yu, H., Li, M., Hang, L., Xu, X., 2020. Apigenin protects mouse retina against oxidative damage by regulating the Nrf2 pathway and autophagy. Oxid. Med. Cell. Longev. 2020.
Zimmermann, E., Souto, E.B., Müller, R.H., 2005. Physicochemical investigations on the structure of drug-free and drug-loaded solid lipid nanoparticles (SLN) by means of DSC and 1H NMR. Pharmazie 60 (7), 508–513.